

2001

# Water Distribution Modeling

Thomas M. Walski

*Haestad Methods*

Donald V. Chase

*University of Dayton*, dchase1@udayton.edu

Dragan A. Savic

*University of Exeter*

Follow this and additional works at: [http://ecommons.udayton.edu/cee\\_fac\\_pub](http://ecommons.udayton.edu/cee_fac_pub)



Part of the [Hydraulic Engineering Commons](#), and the [Structural Engineering Commons](#)

---

## eCommons Citation

Walski, Thomas M.; Chase, Donald V.; and Savic, Dragan A., "Water Distribution Modeling" (2001). *Civil and Environmental Engineering and Engineering Mechanics Faculty Publications*. Paper 17.  
[http://ecommons.udayton.edu/cee\\_fac\\_pub/17](http://ecommons.udayton.edu/cee_fac_pub/17)

This Book is brought to you for free and open access by the Department of Civil and Environmental Engineering and Engineering Mechanics at eCommons. It has been accepted for inclusion in Civil and Environmental Engineering and Engineering Mechanics Faculty Publications by an authorized administrator of eCommons. For more information, please contact [frice1@udayton.edu](mailto:frice1@udayton.edu), [mschlangen1@udayton.edu](mailto:mschlangen1@udayton.edu).

---

CHAPTER

2

# Modeling Theory

Model-based simulation is a method for mathematically approximating the behavior of real water distribution systems. To effectively utilize the capabilities of distribution system simulation software and interpret the results produced, the engineer or modeler must understand the mathematical principles involved. This chapter reviews the principles of hydraulics and water quality analysis that are frequently employed in water distribution network modeling software.

## 2.1 FLUID PROPERTIES

Fluids can be categorized as either gases or liquids. The most notable differences between the two states are that liquids are far denser than gases, and gases are highly compressible compared to liquids (liquids are relatively incompressible). The most important fluid properties taken into consideration in a water distribution simulation are specific weight, fluid viscosity, and (to a lesser degree) compressibility.

### Density and Specific Weight

The *density* of a fluid is the mass of the fluid per unit volume. The density of water is 1.94 slugs/ft<sup>3</sup> (1000 kg/m<sup>3</sup>) at standard pressure of 1 atm (1.013 bar) and standard temperature of 32.0 °F (0.0 °C). A change in temperature or pressure will affect the density, although the effects of minor changes are generally insignificant for water modeling purposes.

The property that describes the weight of a fluid per unit volume is called *specific weight*, and is related to density by gravitational acceleration:

$$\gamma = \rho g \quad (2.1)$$

where  $\gamma$  = fluid specific weight ( $M/L^2/T^2$ )  
 $\rho$  = fluid density ( $M/L^3$ )  
 $g$  = gravitational acceleration constant ( $L/T^2$ )

The specific weight of water,  $\gamma$ , at standard pressure and temperature is  $62.4 \text{ lb/ft}^3$  ( $9,806 \text{ N/m}^3$ ).

## Viscosity

Fluid *viscosity* is the property that describes the ability of a fluid to resist deformation due to shear stress. For many fluids, most notably water, viscosity is a proportionality factor relating the velocity gradient to the shear stress, as described by *Newton's Law of Viscosity*:

$$\tau = \mu \frac{dV}{dy} \quad (2.2)$$

where  $\tau$  = shear stress ( $M/L/T^2$ )  
 $\mu$  = absolute (dynamic) viscosity ( $M/L/T$ )  
 $\frac{dV}{dy}$  = time rate of strain ( $1/T$ )

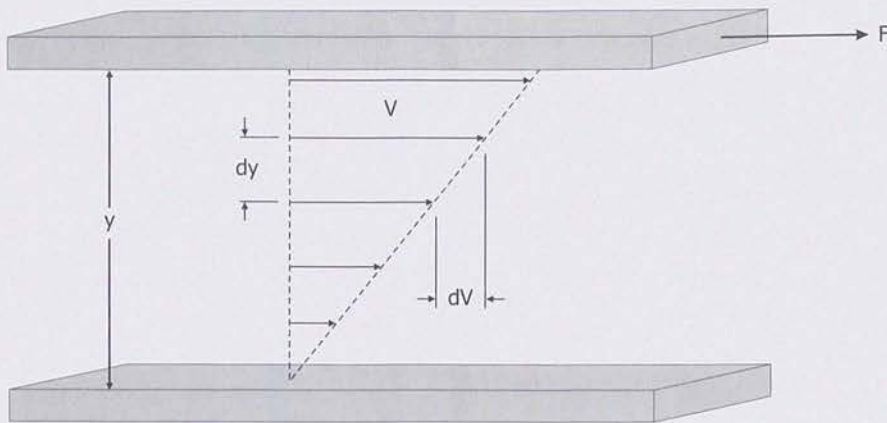
The physical meaning of this equation can be illustrated by considering the two parallel plates shown in Figure 2.1. The space between the plates is filled with a fluid, and the area of the plates is large enough that edge effects can be neglected. The plates are separated by a distance  $y$ , and the top plate is moving at a constant velocity  $V$  relative to the bottom plate. Liquids exhibit an attribute known as the no-slip condition, meaning that they adhere to surfaces they contact. Therefore, if the magnitude of  $V$  and  $y$  are not too large, then the velocity distribution between the two plates is linear.

From *Newton's Second Law of Motion*, for an object to move at a constant velocity, the net external force acting on the object must equal zero. Thus, the fluid must be exerting a force equal and opposite to the force  $F$  on the top plate. This force within the fluid is a result of the shear stress between the fluid and the plate. The velocity at which these forces balance is a function of the velocity gradient normal to the plate and the fluid viscosity, as described by Newton's Law of Viscosity.

Thick fluids, such as syrup and molasses, have high viscosities. Thin fluids, like water and gasoline, have low viscosities. For most fluids, the viscosity will remain constant regardless of the magnitude of the shear stress that is applied to it.

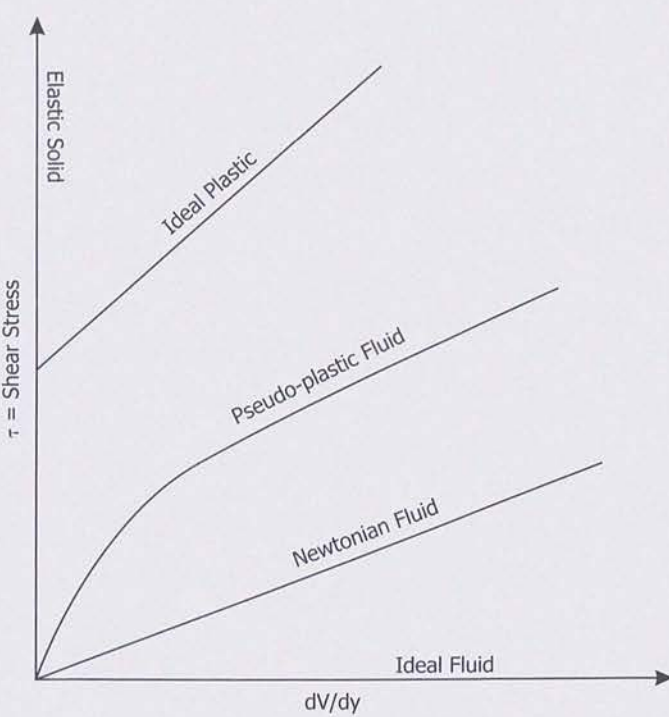
Returning to Figure 2.1, as the velocity of the top plate increases, the shear stresses in the fluid will increase at the same rate. Fluids that exhibit this property conform to *Newton's Law of Viscosity*, and are called *Newtonian fluids*. Water and air are examples of Newtonian fluids. Some types of fluids, like inks and sludge, undergo changes

in viscosity as the shear stress changes. Fluids exhibiting this type of behavior are called *pseudo-plastic fluids*.

**Figure 2.1**

Physical interpretation of Newton's Law of Viscosity

Relationships between the shear stress and the velocity gradient for typical Newtonian and Non-Newtonian fluids are shown in Figure 2.2. Since most distribution system models are intended to simulate water, many of the equations used consider Newtonian fluids only.

**Figure 2.2**

Stress versus strain for plastics and fluids

Viscosity is a function of temperature, but this relationship is different for liquids and gases. In general, viscosity decreases as temperature increases for liquids, and viscosity increases as temperature increases for gases. The temperature variation within water distribution systems, however, is usually quite small, and thus changes in water viscosity are considered negligible for this application. Generally, water distribution system modeling software treats viscosity as a constant [assuming a temperature of 68 °F (20 °C)].

The viscosity derived in Equation 2.2 is referred to as the *absolute viscosity* (or *dynamic viscosity*). For hydraulic formulas related to fluid motion, the relationship between fluid viscosity and fluid density is often expressed as a single variable. This relationship, called the *kinematic viscosity*, is expressed as:

$$\nu = \frac{\mu}{\rho} \quad (2.3)$$

where  $\nu$  = kinematic viscosity ( $L^2/T$ )

Just as there are shear stresses between the plate and the fluid in Figure 2.1, there are shear stresses between the wall of a pipe and the fluid moving through the pipe. The higher the fluid viscosity, the greater the shear stresses that will develop within the fluid, and, consequently, the greater the friction losses along the pipe. Distribution system modeling software packages use fluid viscosity as a factor in estimating the friction losses along a pipe's length. Packages that can handle any fluid require the viscosity and density to be input by the modeler, while models that are developed only for water usually account for the appropriate value automatically.

## Fluid Compressibility

*Compressibility* is a physical property of fluids that relates the volume occupied by a fixed mass of fluid to its pressure. In general, gases are much more compressible than liquids. An air compressor is a simple device that utilizes the compressibility of air to store energy. The compressor is essentially a pump that intermittently forces air molecules into the fixed volume tank attached to it. Each time the compressor turns on, the mass of air, and therefore the pressure within the tank, increases. Thus a relationship exists between fluid mass, volume, and pressure.

This relationship can be simplified by considering a fixed mass of a fluid. Compressibility is then described by defining the fluid's *bulk modulus of elasticity*:

$$E_v = -V \frac{dP}{dV} \quad (2.4)$$

where  $E_v$  = bulk modulus of elasticity ( $M/L/T^2$ )

$P$  = pressure ( $M/L/T^2$ )

$V$  = volume of fluid ( $L^3$ )

All fluids are compressible to some extent. The effects of compression in a water distribution system are very small, and thus the equations used in hydraulic simulations

## Hydraulic Transients

When a pump starts or stops, or a valve is opened or closed, the velocity of water in the pipe changes. However, when flow accelerates or decelerates in a pipe, all of the water in that pipe does not change velocity instantly. It takes time for the water at one end of a pipe to experience the effect of a force applied some distance away. When flow decelerates, the water molecules in the pipe are compressed, and the pressure rises. Conversely, when the flow accelerates, the pressure drops. These changes in pressure travel through the pipe as waves referred to as "hydraulic transients." When a sudden change in velocity occurs, the resulting pressure waves can be strong enough to damage pipes and fittings. This phenomenon is known as water hammer.

The magnitude of the pressure change is determined by the pipe material and wall thickness, fluid compressibility and density, and—most importantly—the magnitude of the change in velocity. The Joukowski equation indicates that, in general, a change in velocity of 1 ft/s can result in a change in head of 100 ft (a 1 m/s change in velocity corresponds to 100 m change in head). Large positive pressures can burst pipes or separate joints, especially at bends. Negative pressure waves can reduce the pressure enough to cause vaporization of water in a process called "column separation." The collapse of these vapor pockets can damage piping. Negative pressures can also draw contaminated groundwater into the distribution system through pipe imperfections.

Transients are damped by pipe friction and the effects of pipe loops that essentially cancel out the pressure waves. Surge tanks and air chambers also have dampening effects. Using slow-opening valves and flywheels on pumps can minimize transients before they occur by reducing the acceleration or deceleration of the water.

Fluid transients tend to be worse in long pipelines carrying water at high velocities. The worst transient effects in water systems are usually brought on by a sudden loss of power to a pump station. Transients can also be caused by a hydrant being shut off too quickly, rapid closing of an automated valve such as an altitude valve, pipe failure, and even normal starting and stopping of pumps.

The unsteady flow equations necessary to model transients are extremely difficult to solve manually in all but the simplest piping configurations. Mathematical models to solve these equations are available, but are considerably more complicated than the types of water distribution system models described in this book.

Transient analysis is a fairly specialized area of hydraulics, and there are several very good references available, including Almeida and Koelle (1992), Chaudhry (1987), Karney (2000), Martin (2000), Thorley (1991), and Wylie and Streeter (1993).

are based on the assumption that the liquids involved are incompressible. With a bulk modulus of elasticity of 410,000 psi ( $2.83 \times 10^6$  kPa) at 68 °F (20 °C), water can safely be treated as incompressible. For instance, a pressure change of over 2,000 psi ( $1.379 \times 10^4$  kPa) results in only a 0.5 percent change in volume.

Although the assumption of incompressibility is justifiable under most conditions, certain hydraulic phenomena are capable of generating pressures high enough that the compressibility of water becomes important. During field operations, a phenomenon known as *water hammer* can develop due to extremely rapid changes in flow (when, for instance, a valve suddenly closes, or a power failure occurs and pumps stop operating). The momentum of the moving fluid can generate pressures large enough that fluid compression and pipe wall expansion can occur, which in turn causes destructive

transient pressure fluctuations to propagate throughout the network. Specialized network simulation software is necessary to analyze these transient pressure effects.

## Vapor Pressure

Consider a closed container that is partly filled with water. The pressure in the container is measured when the water is first added, and again after some time has elapsed. These readings show that the pressure in the container increases during this period. The increase in pressure is due to the evaporation of the water, and the resulting increase in *vapor pressure* above the liquid.

Assuming that temperature remains constant, the pressure will eventually reach a constant value that corresponds to the *equilibrium* or *saturation vapor pressure* of water at that temperature. At this point, the rates of evaporation and condensation are equal.

The saturation vapor pressure increases with increasing temperature. This relationship demonstrates, for example, why the air in humid climates typically feels moister in summer than in winter, and why the boiling temperature of water is lower at higher elevations.

If a sample of water at a pressure of 1 atm and room temperature is heated to 212 °F (100 °C), the water will begin to boil since the vapor pressure of water at that temperature is equal to 1 atm. In a similar vein, if water is held at a temperature of 68 °F (20 °C), and the pressure is decreased to 0.023 atm, the water will also boil.

This concept can be applied in water distribution in cases in which the ambient pressure drops very low. Pump *cavitation* occurs when the fluid being pumped flashes into a vapor pocket, then quickly collapses. For this to happen, the pressure in the pipeline must be equal to or less than the vapor pressure of the fluid. When cavitation occurs it sounds as if gravel is being pumped, and severe damage to pipe walls and pump components can result.

## 2.2 FLUID STATICS AND DYNAMICS

### Static Pressure

*Pressure* can be thought of as a force applied normal, or perpendicular, to a body that is in contact with a fluid. In the English system of units, pressure is expressed in pounds per square foot ( $\text{lb}/\text{ft}^2$ ), but the water industry generally uses  $\text{lb}/\text{in.}^2$ , typically abbreviated as psi. In the SI system, pressure has units of  $\text{N}/\text{m}^2$ , also called a *Pascal*. However, because of the magnitude of pressures occurring in distribution systems, pressure is typically reported in kilo-Pascals (kPa), or 1,000 Pascals.

Pressure varies with depth as illustrated in Figure 2.3. For fluids at rest, the variation of pressure over depth is linear and is called the hydrostatic pressure distribution.

$$P = h\gamma \quad (2.5)$$

where

$P$  = pressure ( $M/L/T^2$ )

$h$  = depth of fluid above datum (L)

$\gamma$  = fluid specific weight ( $M/L^2/T^2$ )

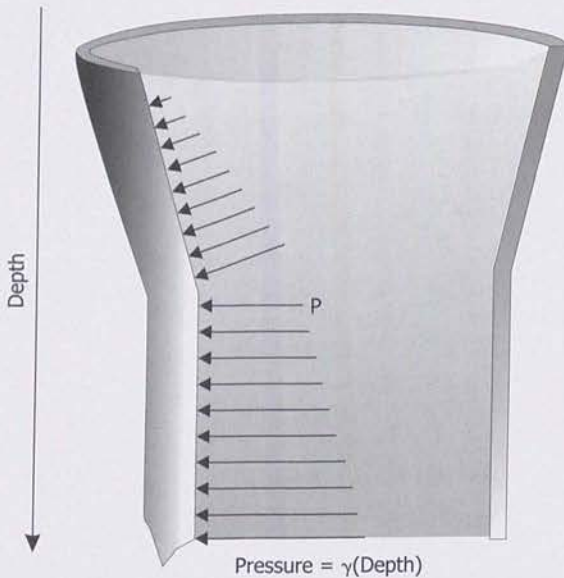


**Figure 2.3**

Static pressure in a standing water column

This equation can be rewritten to find the height of a column of water that can be supported by a given pressure:

$$h = \frac{P}{\gamma} \quad (2.6)$$

The quantity  $P/\gamma$  is called the *pressure head*, which is the energy resulting from water pressure. Recognizing that the specific weight of water in English units is 62.4 lb/ft<sup>3</sup>, a convenient conversion factor can be established for water as 1 psi = 2.31 ft (1 kPa = 0.102 m) of pressure head.

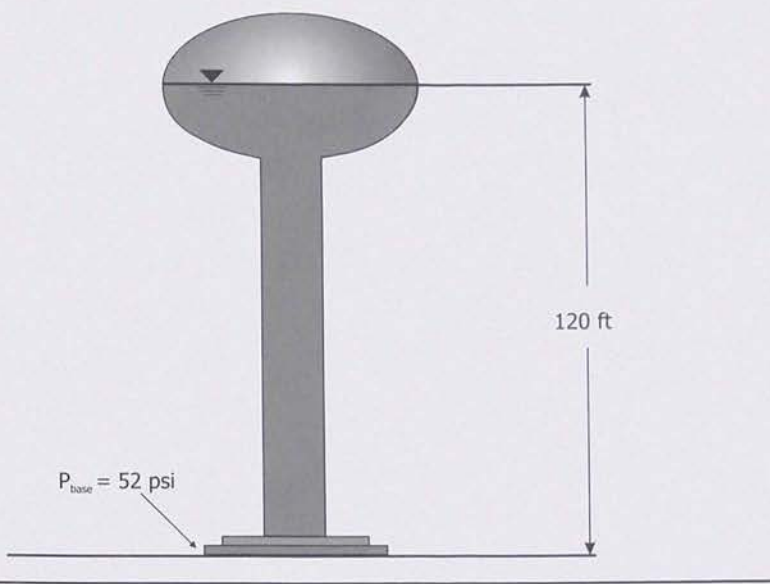
■ **Example - Pressure Calculation** Consider the storage tank in Figure 2.4 in which the water surface elevation is 120 ft above a pressure gage. The pressure at the base of the tank is due to the weight of the column of water directly above it, and can be calculated as follows:

$$P = \gamma h = \frac{62.4 \frac{\text{lb}}{\text{ft}^3} (120 \text{ft})}{\frac{144 \frac{\text{in}^2}{\text{ft}^2}}{}}$$

$$P = 52 \text{ psi}$$

**Figure 2.4**

Storage tank



**Absolute Pressure and Gage Pressure.** Pressure at a given point is due to the weight of the fluid above that point. The weight of the earth's atmosphere produces a pressure, referred to as *atmospheric pressure*. Although the actual atmospheric pressure will depend upon elevation and weather, standard atmospheric pressure at sea level is 1 atm (14.7 psi or 101 kPa).

Two types of pressure are commonly used in hydraulics, absolute pressure and gage pressure. *Absolute pressure* is the pressure measured with absolute zero (a perfect vacuum) as its datum, while *gage pressure* is the pressure measured with atmospheric pressure as its datum. The two are related to one another as shown in Equation 2.7. Note that when a pressure gage located at the earth's surface is open to the atmosphere, it registers zero on its dial. If the gage pressure is negative (that is, the pressure is below atmospheric), then the negative pressure is called a vacuum.

$$P_{abs} = P_{gage} + P_{atm} \quad (2.7)$$

where  $P_{abs}$  = absolute pressure ( $\text{M/L/T}^2$ )  
 $P_{gage}$  = gage pressure ( $\text{M/L/T}^2$ )  
 $P_{atm}$  = atmospheric pressure ( $\text{M/L/T}^2$ )

In most hydraulic applications, including water distribution systems analysis, gage pressure is used. Using absolute pressure has little value, since doing so would simply result in all the gage pressures being incremented by atmospheric pressure. Additionally, gage pressure is often more intuitive because people do not typically consider atmospheric effects when thinking about pressure.

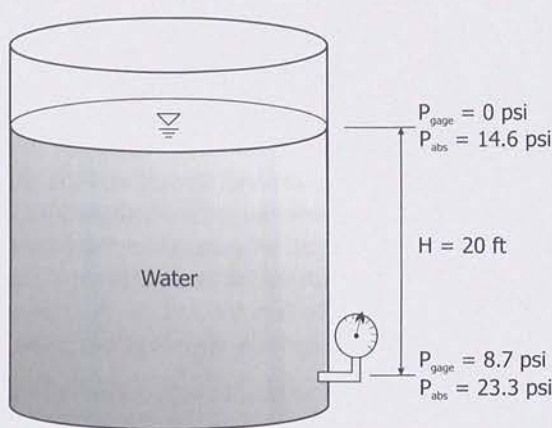


**Figure 2.5**  
Gage versus absolute pressure

## Velocity and Flow Regime

The velocity profile of a fluid as it flows through a pipe is not constant across the diameter. Rather, the velocity of a fluid particle depends upon where the fluid particle is located with respect to the pipe wall. In most cases, hydraulic models deal with the average velocity in a cross-section of pipeline, which can be found using the following formula:

$$V = \frac{Q}{A} \quad (2.8)$$

where       $V$  = average fluid velocity ( $L/T$ )  
 $Q$  = pipeline flow rate ( $L^3/T$ )  
 $A$  = cross-sectional area of pipeline ( $L^2$ )

The cross-sectional area of a circular pipe can be directly computed from the diameter  $D$ , so the velocity equation can be rewritten as:

$$V = \frac{4Q}{\pi D^2} \quad (2.9)$$

where       $D$  = diameter ( $L$ )

For water distribution systems in which diameter is measured in inches and flow is measured in gallons per minute, the equation simplifies to:

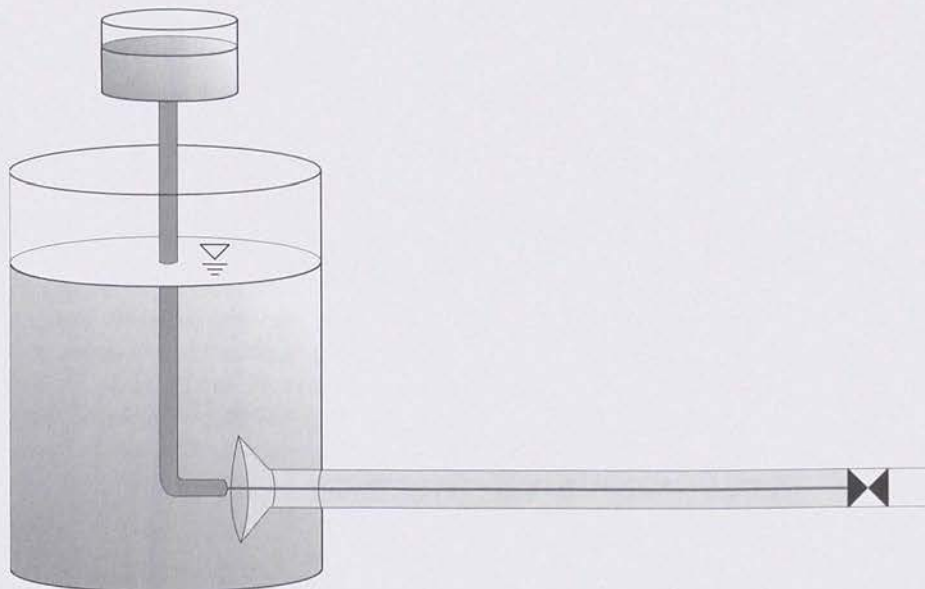
$$V = 0.41 \frac{Q}{D^2} \quad (2.10)$$

where       $V$  = average fluid velocity ( $ft/s$ )  
 $Q$  = pipeline flow rate ( $gpm$ )  
 $D$  = diameter ( $in.$ )

**Reynolds Number.** In the late 1800s, an English scientist named Osborne Reynolds conducted experiments on fluid passing through a glass tube. His experimental setup looked much like the one in Figure 2.6 (Streeter, Wylie, and Bedford, 1998). The experimental apparatus was designed to establish the flow rate through a long glass tube (meant to simulate a pipeline) and to allow dye (from a smaller tank) to flow into the liquid. He noticed that at very low flow rates, the dye stream remained intact with a distinct interface between the dye stream and the fluid surrounding it. Reynolds referred to this condition as *laminar flow*. At slightly higher flow rates, the dye stream began to waver a bit, and there was some blurring between the dye stream and the surrounding fluid. He called this condition *transitional flow*. At even higher flows, the dye stream was completely broken up, and the dye mixed completely with the surrounding fluid. Reynolds referred to this regime as *turbulent flow*.

When Reynolds conducted the same experiment using different fluids, he noticed that the condition under which the dye stream remained intact not only varied with the flow rate through the tube, but also with the fluid density and viscosity, and the diameter of the tube.

**Figure 2.6**  
Experimental apparatus used to determine Reynolds number



Based on experimental evidence gathered by Reynolds and dimensional analysis, a dimensionless number can be computed and used to characterize flow regime. Conceptually, the *Reynolds number* can be thought of as the ratio between inertial and viscous forces in a fluid. The Reynolds number for full flowing circular pipes can be found using the following equation:

$$Re = \frac{VD\rho}{\mu} = \frac{VD}{v} \quad (2.11)$$

where  $Re$  = Reynolds Number  
 $D$  = pipeline diameter (L)  
 $\rho$  = fluid density ( $M/L^3$ )  
 $\mu$  = absolute viscosity ( $M/L/T$ )  
 $v$  = kinematic viscosity ( $L^2/T$ )

The ranges of the Reynolds Number that define the three flow regimes are shown in Table 2.1. The flow of water through municipal water systems is almost always turbulent, except in the periphery where water demand is low and intermittent, and may result in laminar and stagnant flow conditions.

**Table 2.1** Reynolds Number for various flow regimes

Flow Regime	Reynolds Number
Laminar	< 2000
Transitional	2000-4000
Turbulent	> 4000

**Velocity Profiles.** Due to the shear stresses along the walls of a pipe, the velocity in a pipeline is not uniform over the pipe diameter. Rather, the fluid velocity is zero at the pipe wall. Fluid velocity increases with distance from the pipe wall, with the maximum occurring along the centerline of the pipe. Figure 2.7 illustrates the variation of fluid velocity within a pipe, also called the *velocity profile*.

The shape of the velocity profile will vary depending on whether the flow regime is laminar or turbulent. In laminar flow, the fluid particles travel in parallel layers or lamina, producing very strong shear stresses between adjacent layers, and causing the dye streak in Reynolds' experiment to remain intact. Mathematically, the velocity profile in laminar flow is shaped like a parabola as shown in Figure 2.7. In laminar flow, the head loss through a pipe segment is primarily a function of the fluid viscosity, not the internal pipe roughness.

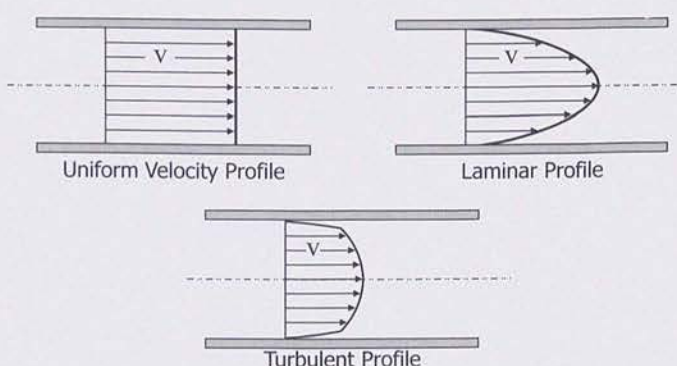


**Figure 2.7**  
Velocity profiles for different flow regimes

Turbulent flow is characterized by eddies that produce random variations in the velocity profiles. Although the velocity profile of turbulent flow is more erratic than that of

laminar flow, the mean velocity profile actually exhibits less variation across the pipe. The velocity profiles for both turbulent and laminar flows are shown in Figure 2.7.

### 2.3 ENERGY CONCEPTS

Fluids possess energy in three forms. The amount of energy depends upon the fluid's movement (*kinetic energy*), elevation (*potential energy*), and pressure (*pressure energy*). In a hydraulic system, a fluid can have all three types of energy associated with it simultaneously. The total energy associated with a fluid per unit weight of the fluid is called *head*. The kinetic energy is called *velocity head* ( $V^2/2g$ ), the potential energy is called *elevation head* ( $Z$ ), and the internal pressure energy is called *pressure head* ( $P/\gamma$ ). While typical units for energy are foot-pounds (Joules), the units of total head are feet (meters).

$$H = Z + \frac{P}{\gamma} + \frac{V^2}{2g} \quad (2.12)$$

where

$H$  = total head (L)

$Z$  = elevation above datum (L)

$P$  = pressure ( $M/L/T^2$ )

$\gamma$  = fluid specific weight ( $M/L^2/T^2$ )

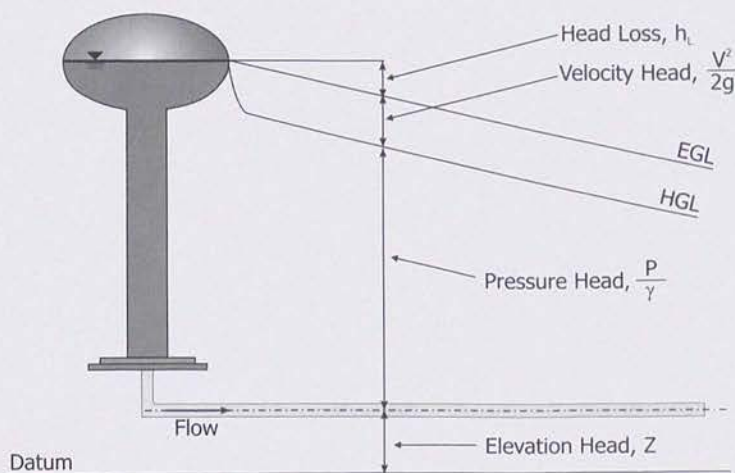
$V$  = velocity ( $L/T$ )

$g$  = gravitational acceleration constant ( $L/T^2$ )

Each point in the system has a unique head associated with it. A line plotted of total head versus distance through a system is called the *energy grade line* (EGL). The sum of the elevation head and pressure head yields the *hydraulic grade line* (HGL), which corresponds to the height that water will rise vertically in a tube attached to the pipe and open to the atmosphere. Figure 2.8 shows the EGL and HGL for a simple pipeline.

**Figure 2.8**

Energy and hydraulic grade lines



In most water distribution applications, the elevation and pressure head terms are much greater than the velocity head term. For this reason, velocity head is often ignored, and modelers work in terms of hydraulic grades rather than energy grades. Therefore, given a datum elevation and a hydraulic grade line, the pressure can be determined as:

$$P = \gamma(HGL - Z) \quad (2.13)$$

where  $HGL$  = hydraulic grade line (L)

## Energy Losses

Energy losses, also called head losses, are generally the result of two mechanisms:

- Friction along the pipe walls
- Turbulence due to changes in streamlines through fittings and appurtenances

Head losses along the pipe wall are called *friction losses* or head losses due to friction, while losses due to turbulence within the bulk fluid are called *minor losses*.

## 2.4 FRICTION LOSSES

When a liquid flows through a pipeline, shear stresses develop between the liquid and the pipe wall. This shear stress is a result of friction, and its magnitude is dependent upon the properties of the fluid that is passing through the pipe, the speed at which it is moving, the internal roughness of the pipe, and the length and diameter of the pipe.

Consider, for example, the pipe segment shown in Figure 2.9. A force balance on the fluid element contained within a pipe section can be used to form a general expression describing the head loss due to friction. Note the forces in action:

- Pressure difference between Sections 1 and 2
- The weight of the fluid volume contained between Sections 1 and 2
- The shear at the pipe walls between Sections 1 and 2

Assuming the flow in the pipeline has a constant velocity (that is, acceleration is equal to zero), the system can be balanced based on the pressure difference, gravitational forces, and shear forces.

$$P_1 A_1 - P_2 A_2 - \bar{A} L \gamma \sin(\alpha) - \tau_o N L = 0 \quad (2.14)$$

where  $P_1$  = pressure at section 1 ( $M/L/T^2$ )

$A_1$  = cross-sectional area of section 1 ( $L^2$ )

$P_2$  = pressure at section 2 ( $M/L/T^2$ )

$A_2$  = cross-sectional area of section 2 ( $L^2$ )

$\bar{A}$  = average area between section 1 and section 2 ( $L^2$ )

$L$  = distance between section 1 and section 2 (L)

$\gamma$  = fluid specific weight ( $M/L^3/T^2$ )

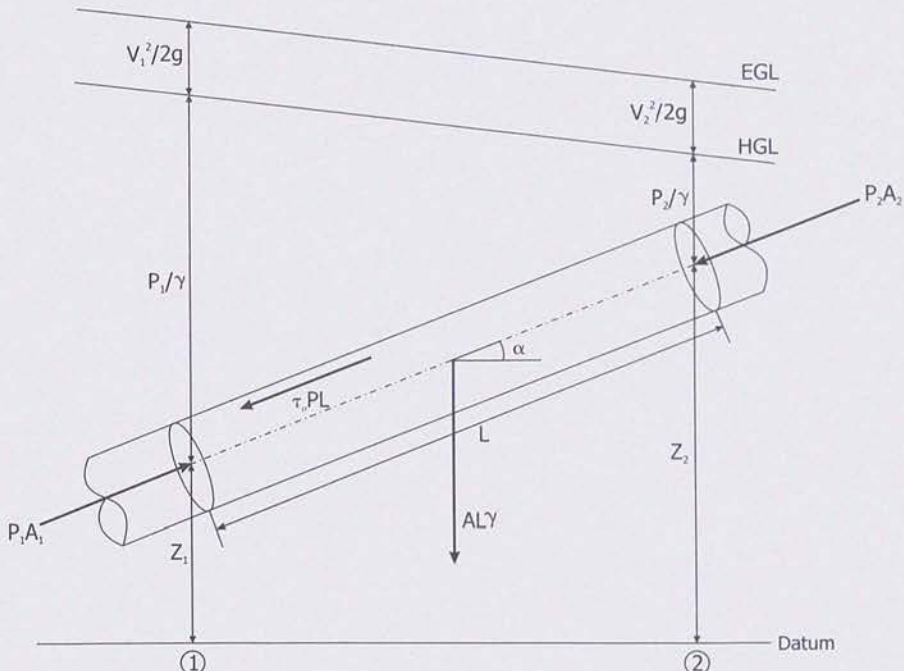
$\alpha$  = angle of the pipe to horizontal

$\tau_o$  = shear stress along pipe wall ( $M/L/T^2$ )

$N$  = perimeter of pipeline cross-section (L)

**Figure 2.9**

Free body diagram of water flowing in an inclined pipe



The last term on the left side of Equation 2.14 represents the friction losses along the pipe wall between the two sections. By recognizing that  $\sin(\alpha) = (Z_2 - Z_1)/L$ , the equation for head loss due to friction can be rewritten to obtain the following equation. (Note that the velocity head is not considered in this case because the pipe diameters, and therefore the velocity heads, are the same.)

$$h_L = \tau_o \frac{NL}{\gamma A} = \left( \frac{P_1}{\gamma} + Z_1 \right) - \left( \frac{P_2}{\gamma} + Z_2 \right) \quad (2.15)$$

where  $h_L$  = head loss due to friction (L)

$Z_1$  = elevation of centroid of section 1 (L)

$Z_2$  = elevation of centroid of section 2 (L)

Recall that the shear stresses in a fluid can be found analytically for laminar flow using Newton's Law of Viscosity. Shear stress is a function of the viscosity and velocity gradient of the fluid, the fluid specific weight (or density), and the diameter of the pipeline. The roughness of the pipe wall is also a factor (that is, the rougher the pipe wall, the larger the shear stress). Combining all of these factors, it can be seen that:

$$\tau_o = F(\rho, \mu, V, D, \epsilon) \quad (2.16)$$

where  $\rho$  = fluid density ( $M/L^3$ )  
 $\mu$  = absolute viscosity ( $M/L/T$ )  
 $V$  = average fluid velocity ( $L/T$ )  
 $D$  = diameter ( $L$ )  
 $\epsilon$  = index of internal pipe roughness ( $L$ )

## Darcy-Weisbach

Using dimensional analysis, the *Darcy-Weisbach formula* was developed. The formula is an equation for head loss expressed in terms of the variables listed in Equation 2.16, as follows (note that head loss is expressed with units of length):

$$h_L = f \frac{LV^2}{D^2 g} = \frac{8fLQ^2}{gD^5 \pi^2} \quad (2.17)$$

where  $f$  = Darcy-Weisbach friction factor  
 $g$  = gravitational acceleration constant ( $L/T^2$ )  
 $Q$  = pipeline flow rate ( $L^3/T$ )

The Darcy-Weisbach *friction factor*,  $f$ , is a function of the same variables as wall shear stress (Equation 2.16). Again using dimensional analysis, a functional relationship for the friction factor can be developed:

$$f = F\left(\frac{VD\rho}{\mu}, \frac{\epsilon}{D}\right) = F\left(Re, \frac{\epsilon}{D}\right) \quad (2.18)$$

where  $Re$  = Reynolds Number

The Darcy-Weisbach friction factor is dependent upon the velocity, density, and viscosity of the fluid; the size of the pipe in which the fluid is flowing; and the internal roughness of the pipe. The fluid velocity, density, viscosity, and pipe size are expressed in terms of the Reynolds Number. The internal roughness is expressed in terms of a variable called the *relative roughness*, which is the internal pipe roughness ( $\epsilon$ ) divided by the pipe diameter ( $D$ ).

In the early 1930s, the German researcher Nikuradse performed an experiment that would become fundamental in head loss determination (Nikuradse, 1932). He glued uniformly sized sand grains to the insides of three pipes of different sizes. His experiments showed that the curve of  $f$  versus  $Re$  is smooth for the same values of  $\epsilon/D$ . Partly because of Nikuradse's sand grain experiments, the quantity  $\epsilon$  is called the *equivalent sand grain roughness* of the pipe. Table 2.2 provides values of  $\epsilon$  for various materials.

Other researchers conducted experiments on artificially roughened pipes to generate data describing pipe friction factors for a wide range of relative roughness values.

**Table 2.2** Equivalent sand grain roughness for various pipe materials

Material	Equivalent Sand Roughness, $\epsilon$	
	(ft)	(mm)
Copper, brass	$1 \times 10^{-4} - 3 \times 10^{-3}$	$3.05 \times 10^{-2} - 0.9$
Wrought iron, steel	$1.5 \times 10^{-4} - 8 \times 10^{-3}$	$4.6 \times 10^{-2} - 2.4$
Asphalted cast iron	$4 \times 10^{-4} - 7 \times 10^{-3}$	0.1 - 2.1
Galvanized iron	$3.3 \times 10^{-4} - 1.5 \times 10^{-2}$	0.102 - 4.6
Cast iron	$8 \times 10^{-4} - 1.8 \times 10^{-2}$	0.2 - 5.5
Concrete	$10^{-3}$ to $10^{-2}$	0.3 to 3.0
Uncoated Cast Iron	$7.4 \times 10^{-4}$	0.226
Coated Cast Iron	$3.3 \times 10^{-4}$	0.102
Coated Spun Iron	$1.8 \times 10^{-4}$	$5.6 \times 10^{-2}$
Cement	$1.3 \times 10^{-3} - 4 \times 10^{-3}$	0.4 - 1.2s
Wrought Iron	$1.7 \times 10^{-4}$	$5 \times 10^{-2}$
Uncoated Steel	$9.2 \times 10^{-4}$	$2.8 \times 10^{-2}$
Coated Steel	$1.8 \times 10^{-4}$	$5.8 \times 10^{-2}$
Wood Stave	$6 \times 10^{-4} - 3 \times 10^{-3}$	0.2 - 0.9
PVC	$5 \times 10^{-6}$	$1.5 \times 10^{-3}$

Compiled from Lamont (1981), Moody (1944), and Mays (1999)

**Colebrook-White Equation and the Moody Diagram.** Numerous formulas exist that relate the friction factor to the Reynolds Number and relative roughness. One of the earliest and most popular of these formulas is the *Colebrook-White equation*:

$$\frac{1}{\sqrt{f}} = -0.86 \ln \left( \frac{\epsilon}{3.7D} + \frac{2.51}{Re \sqrt{f}} \right) \quad (2.19)$$

The difficulty with using the Colebrook-White equation is that it is an implicit function of the friction factor ( $f$  is found on both sides of the equation). Typically, the equation is solved by iterating through assumed values of  $f$  until both sides are equal.

The *Moody diagram*, shown in Figure 2.10, was developed from the Colebrook-White equation as a graphical solution for the Darcy-Weisbach friction factor.

It is interesting to note that for laminar flow (low  $Re$ ) the friction factor is a linear function of the Reynolds Number, while in the fully turbulent range (high  $\epsilon/D$  and high  $Re$ ) the friction factor is only a function of the relative roughness. This difference occurs because the effect of roughness is negligible for laminar flow, while for very turbulent flow the viscous forces become negligible.

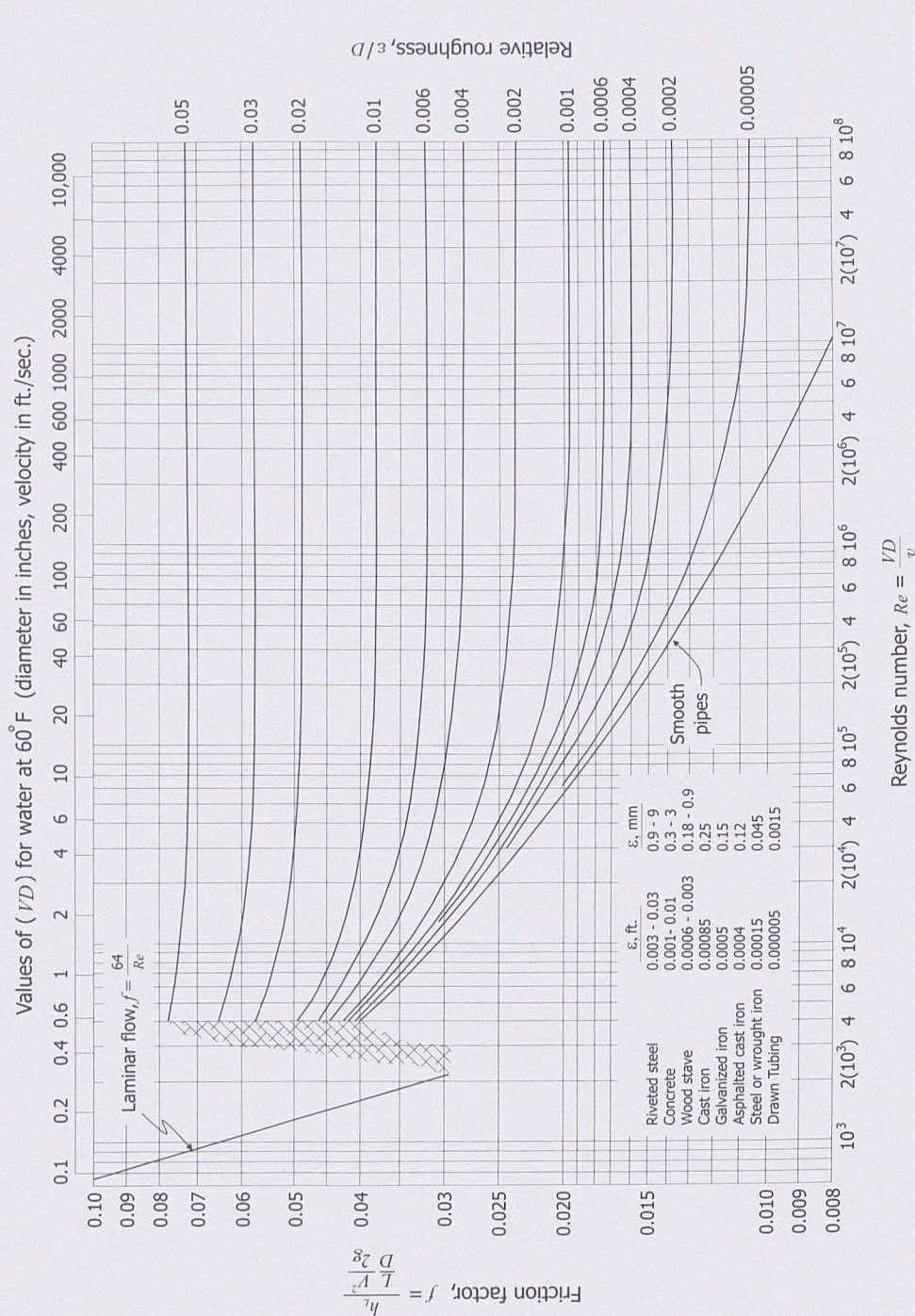


**Figure 2.10**  
Moody diagram

From L. F. Moody, "Friction Factors for Pipe Flow," Trans. A.S.M.E., Vol. 66, 1944, used with permission.

**Swamee-Jain Formula.** Much easier to solve than the iterative Colebrook-White formula, the formula developed by Swamee and Jain (1976) also approximates the Darcy-Weisbach friction factor. This equation is an explicit function of the Reynolds Number and the relative roughness, and is accurate to within about one percent of the Colebrook-White equation over a range of:

$$4 \times 10^3 \leq Re \leq 1 \times 10^8 \text{ and}$$

$$1 \times 10^{-6} \leq \epsilon/D \leq 1 \times 10^{-2}$$

$$f = \frac{1.325}{\left[ \ln \left( \frac{\epsilon}{3.7D} + \frac{5.74}{Re^{0.9}} \right) \right]^2} \quad (2.20)$$

Because of its relative simplicity and reasonable accuracy, most water distribution system modeling software packages use the *Swamee-Jain formula* to compute the friction factor.

## Hazen-Williams

Another frequently used head loss expression, particularly in North America, is the *Hazen-Williams formula* (Williams and Hazen, 1920; ASCE, 1992):

$$h_L = \frac{C_f L}{C^{1.852} D^{4.87}} Q^{1.852} \quad (2.21)$$

where  $h_L$  = head loss due to friction (ft, m)  
 $L$  = distance between section 1 and 2 (ft, m)  
 $C$  = Hazen-Williams C-factor  
 $D$  = diameter (ft, m)  
 $Q$  = pipeline flow rate (cfs,  $m^3/s$ )  
 $C_f$  = unit conversion factor (4.73 English, 10.7 SI)

The Hazen-Williams formula uses many of the same variables as Darcy-Weisbach, but instead of using a friction factor, the Hazen-Williams formula uses a pipe carrying capacity factor,  $C$ . Higher C-factors represent smoother pipes (with higher carrying capacities) and lower C-factors describe rougher pipes. Table 2.3 shows typical C-factors for various pipe materials, based on Lamont (1981).

Lamont found that it was not possible to develop a single correlation between pipe age and C-factor and that instead, the decrease in C-factor also depended heavily on the corrosiveness of the water being carried. He developed four separate “trends” in carrying capacity loss depending on the “attack” of the water on the pipe. Trend 1, slight attack, corresponded to water that was only mildly corrosive. Trend 4, severe attack, corresponded to water that would rapidly attack cast iron pipe. As can be seen from Table 2.3, the extent of attack can significantly affect C-factor. Testing pipes to determine the loss of carrying capacity is discussed further on page 178.

From a purely theoretical standpoint, the C-factor of a pipe should vary with the flow velocity under turbulent conditions. Equation 2.22 can be used to adjust the C-factor

**Table 2.3** C-factors for various pipe materials.

Type of Pipe	C-factor Values for Discrete Pipe Diameters					
	1.0 in. (2.5 cm)	3.0 in. (7.6 cm)	6.0 in. (15.2 cm)	12 in. (30 cm)	24 in. (61 cm)	48 in. (122 cm)
Uncoated cast iron - smooth and new	121	125	130	132	134	
Coated cast iron - smooth and new	129	133	138	140	141	
30 years old						
Trend 1 - slight attack	100	106	112	117	120	
Trend 2 - moderate attack	83	90	97	102	107	
Trend 3 - appreciable attack	59	70	78	83	89	
Trend 4 - severe attack	41	50	58	66	73	
60 years old						
Trend 1 - slight attack	90	97	102	107	112	
Trend 2 - moderate attack	69	79	85	92	96	
Trend 3 - appreciable attack	49	58	66	72	78	
Trend 4 - severe attack	30	39	48	56	62	
100 years old						
Trend 1 - slight attack	81	89	95	100	104	
Trend 2 - moderate attack	61	70	78	83	89	
Trend 3 - appreciable attack	40	49	57	64	71	
Trend 4 - severe attack	21	30	39	46	54	
Miscellaneous						
Newly scraped mains	109	116	121	125	127	
Newly brushed mains	97	104	108	112	115	
Coated spun iron - smooth and new	137	142	145	148	148	
Old - take as coated cast iron of same age						
Galvanized iron - smooth and new	120	129	133			
Wrought iron - smooth and new	129	137	142			
Coated steel - smooth and new	129	137	142	145	148	148
Uncoated Steel - smooth and new	134	142	145	147	150	150
Coated asbestos cement - clean		147	149	150	152	
Uncoated asbestos cement - clean		142	145	147	150	
Spun cement-lined and spun bitumen-lined - clean		147	149	150	152	153
Smooth pipe (including lead, brass, copper, polyethylene, and PVC) - clean	140	147	149	150	152	153
PVC wavy - clean	134	142	145	147	150	150
Concrete - Scobey						
Class 1 - $C_s = 0.27$ ; clean	69	79	84	90	95	
Class 2 - $C_s = 0.31$ ; clean	95	102	106	110	113	
Class 3 - $C_s = 0.345$ ; clean	109	116	121	125	127	
Class 4 - $C_s = 0.37$ ; clean	121	125	130	132	134	
Best - $C_s = 0.40$ ; clean	129	133	138	140	141	
Tate relined pipes - clean		109	116	121	125	127
Prestressed concrete pipes - clean				147	150	150

Lamont (1981)

for different velocities, but the effects of this correction are usually minimal. A two-fold increase in the flow velocity correlates to an apparent five percent decrease in the roughness factor. This difference is usually within the error range for the roughness estimate in the first place, so most engineers assume the C-factor remains constant regardless of flow (Walski, 1984). However, if C-factor tests are done at very high velocities (e.g., >10 ft/s), then a significant error can result when the resulting C-factors are used to predict head loss at low velocities.

$$C = C_o \left( \frac{V_o}{V} \right)^{0.081} \quad (2.22)$$

where       $C$  = velocity adjusted C-Factor  
 $C_o$  = reference C-Factor  
 $V_o$  = reference value of velocity at which  $C_o$  was determined (L/T)

## Manning Equation

Another head loss expression more typically associated with open channel flow is the *Manning equation*:

$$h_L = \frac{C_f L (nQ)^2}{D^{5.33}} \quad (2.23)$$

where       $n$  = Manning roughness coefficient  
 $C_f$  = unit conversion factor (4.66 English, 5.29 SI)

As with the previous head loss expressions, the head loss computed using Manning equation is dependent upon the pipe length and diameter, the discharge or flow through the pipe, and a *roughness coefficient*. In this case, a higher value of  $n$  represents a higher internal pipe roughness. Table 2.4 provides typical Manning's roughness coefficients for commonly used pipe materials.

**Table 2.4** Manning's roughness values

Material	Manning Coefficient	Material	Manning Coefficient
Asbestos cement	.011	Corrugated metal	.022
Brass	.011	Galvanized iron	.016
Brick	.015	Lead	.011
Cast iron, new	.012	Plastic	.009
Concrete		Steel	
Steel forms	.011	Coal-tar enamel	.010
Wooden forms	.015	New unlined	.011
Centrifugally spun	.013	Riveted	.019
Copper	.011	Wood stave	.012

## Comparison of Friction Loss Methods

Most hydraulic models have features that allow the user to select from the Darcy-Weisbach, Hazen-Williams, or Manning head loss formulas, depending on the nature of the problem and the user's preferences.

The Darcy-Weisbach formula is a more physically-based equation, derived from the basic governing equations of Newton's Second Law. With appropriate fluid viscosities and densities, Darcy-Weisbach can be used to find the head loss in a pipe for any Newtonian fluid in any flow regime.

The Hazen-Williams and Manning formulas, on the other hand, are empirically-based expressions (meaning that they were developed from experimental data), and generally only apply to water under turbulent flow conditions.

The Hazen-Williams formula is the predominant equation used in the U.S., while Darcy-Weisbach is predominant in Europe. The Manning formula is not typically used for water distribution modeling, however, it is sometimes used in Australia. Table 2.5 presents these three equations in several common unit configurations. These equations solve for the friction slope ( $S_f$ ), which is the head loss per unit length of pipe.

**Table 2.5** Friction loss equations in typical units

Equation	Q (m <sup>3</sup> /s); D (m)	Q (cfs); D (ft)	Q (gpm); D (in.)
Darcy-Weisbach	$S_f = \frac{0.083fQ^2}{D^5}$	$S_f = \frac{0.025fQ^2}{D^5}$	$S_f = \frac{0.031fQ^2}{D^5}$
Hazen-Williams	$S_f = \frac{10.7\left(\frac{Q}{C}\right)^{1.852}}{D^{4.87}}$	$S_f = \frac{4.73\left(\frac{Q}{C}\right)^{1.852}}{D^{4.87}}$	$S_f = \frac{10.5\left(\frac{Q}{C}\right)^{1.852}}{D^{4.87}}$
Manning	$S_f = \frac{10.3(nQ)^2}{D^{5.33}}$	$S_f = \frac{4.66(nQ)^2}{D^{5.33}}$	$S_f = \frac{13.2(nQ)^2}{D^{5.33}}$

Compiled from ASCE (1975) and ASCE/WEF (1982)

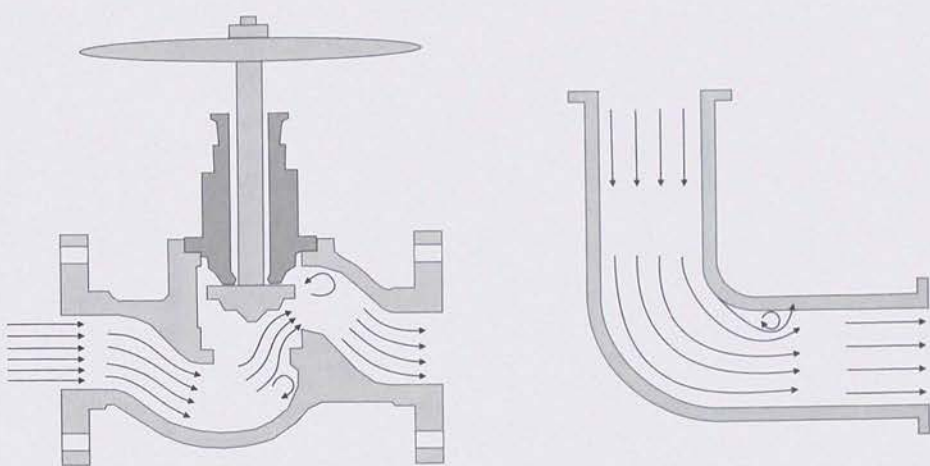
## 2.5 MINOR LOSSES

Head losses also occur at valves, tees, bends, reducers, and other *appurtenances* within the piping system. These losses, called *minor losses*, are due to turbulence within the bulk flow as it moves through fittings and bends. Figure 2.11 illustrates the turbulent eddies that develop within the bulk flow as it travels through a valve and a 90-degree bend.

Head loss due to minor losses can be computed by multiplying a *minor loss coefficient* by the velocity head as shown in Equation 2.24.

**Figure 2.11**

Valve and bend cross-sections generating minor losses



$$h_m = K_L \frac{V^2}{2g} = K_L \frac{Q^2}{2gA^2} \quad (2.24)$$

where  $h_m$  = head loss due to minor losses (L)

$K_L$  = minor loss coefficient

$V$  = velocity (L/T)

$g$  = gravitational acceleration constant (L/T<sup>2</sup>)

$A$  = cross-sectional area (L<sup>2</sup>)

$Q$  = flow rate (L<sup>3</sup>/T)

Minor loss coefficients are found experimentally, and data are available for many different types of fittings and appurtenances. Table 2.6 provides a list of minor loss coefficients associated with several of the most commonly used fittings. More thorough treatments of minor loss coefficients can be found in Crane (1972), Miller (1978), and Idelchik (1999).

For water distribution systems, minor losses are generally much smaller than the head losses due to friction (hence the term "minor" loss). For this reason, many modelers frequently choose to neglect minor losses. In some cases, however, such as at pump stations or valve manifolds where there may be more fittings and higher velocities, minor losses can play a significant role in the piping system under consideration.

Like pipe roughness coefficients, minor head loss coefficients will vary somewhat with velocity. For most practical network problems, however, the minor loss coefficient is treated as constant.

**Table 2.6** Minor loss coefficients

Fitting	$K_L$	Fitting	$K_L$
Pipe Entrance		90° smooth bend	
Bellmouth	0.03-0.05	Bend radius/D = 4	0.16-0.18
Rounded	0.12-0.25	Bend radius/D = 2	0.19-0.25
Sharp Edged	0.50	Bend radius/D = 1	0.35-0.40
Projecting	0.78	Mitered bend	
Contraction - sudden		$\theta = 15^\circ$	0.05
$D_2/D_1=0.80$	0.18	$\theta = 30^\circ$	0.10
$D_2/D_1=0.50$	0.37	$\theta = 45^\circ$	0.20
$D_2/D_1=0.20$	0.49	$\theta = 60^\circ$	0.35
Contraction - conical		$\theta = 90^\circ$	0.80
$D_2/D_1=0.80$	0.05	Tee	
$D_2/D_1=0.50$	0.07	Line flow	0.30-0.40
$D_2/D_1=0.20$	0.08	Branch flow	0.75-1.80
Expansion - sudden		Cross	
$D_2/D_1=0.80$	0.16	Line flow	0.50
$D_2/D_1=0.50$	0.57	Branch flow	0.75
$D_2/D_1=0.20$	0.92	45° Wye	
Expansion - conical		Line flow	0.30
$D_2/D_1=0.80$	0.03	Branch flow	0.50
$D_2/D_1=0.50$	0.08	Check valve - conventional	4.0
$D_2/D_1=0.20$	0.13	Check valve - clearway	1.5
Gate valve - open	0.39	Check valve - ball	4.5
3/4 open	1.10	Butterfly valve - open	1.2
1/2 open	4.8	Cock - straight through	0.5
1/4 open	27	Foot valve - hinged	2.2
Globe valve - open	10	Foot valve - poppet	12.5
Angle valve - open	4.3		

Walski (1984)

## Valve Coefficient

Most valve manufacturers can provide a chart of percent opening versus valve coefficient ( $C_v$ ), which can be related to the minor loss ( $K_L$ ) using the following formula.

$$K_L = C_f D^4 / C_v^2 \quad (2.25)$$

where  $D$  = diameter (in., m)

$C_v$  = valve coefficient [ $\text{gpm}/(\text{psi})^{0.5}$ ,  $(\text{m}^3/\text{s})/(\text{kPa})^{0.5}$ ]

$C_f$  = unit conversion factor (880 English, 1.22 SI)

**Figure 2.12**

48-in. elbow fitting



### Equivalent Pipe Length

Rather than including minor loss coefficients directly, a modeler may choose to adjust the modeled pipe length to account for minor losses by adding an equivalent length of pipe for each minor loss. Given the minor loss coefficient for a valve or fitting, the equivalent length of pipe to give the same head loss can be calculated as:

$$L_e = \frac{K_L D}{f} \quad (2.26)$$

where       $L_e$  = equivalent length of pipe (L)  
 $D$  = diameter of equivalent pipe (L)  
 $f$  = Darcy-Weisbach friction factor

The practice of assigning equivalent pipe lengths was typically used when hand calculations were more common, because it could save time for the overall analysis of a pipeline. With modern computer modeling techniques, this is no longer a widespread practice. Because it is now so easy to use minor loss coefficients directly within a hydraulic model, the process of determining equivalent lengths is actually less efficient. In addition, use of equivalent pipe lengths can unfavorably affect the travel time predictions that are important in many water quality calculations.

## 2.6 RESISTANCE COEFFICIENTS

Many related expressions for head loss have been developed. They can be mathematically generalized with the introduction of a variable referred to as a *resistance coefficient*. This format allows the equation to remain essentially the same regardless of which friction method is used, making it ideal for hydraulic modeling.

$$h_L = K_p Q^z \quad (2.27)$$

where  $h_L$  = head loss due to friction (L)  
 $K_p$  = pipe resistance coefficient ( $T'/L^{3z+1}$ )  
 $Q$  = pipeline flow rate ( $L^3/T$ )  
 $z$  = exponent on flow term

Equations for computing  $K_p$  with the various head loss methods are given below.

### Darcy-Weisbach

$$K_p = f \frac{L}{2gA^z D} \quad (2.28)$$

where  $f$  = Darcy-Weisbach friction factor  
 $L$  = length of pipe (L)  
 $D$  = pipe diameter (L)  
 $A$  = cross-sectional area of pipeline ( $L^2$ )  
 $z = 2$

### Hazen-Williams

$$K_p = \frac{C_f L}{C^z D^{4.87}} \quad (2.29)$$

where  $K_p$  = pipe resistance coefficient ( $s^z/\text{ft}^{3z-1}$ ,  $s'/\text{m}^{3z-1}$ )  
 $L$  = length of pipe (ft, m)  
 $C$  = C-factor with velocity adjustment  
 $z = 1.852$   
 $D$  = pipe diameter (ft, m)  
 $C_f$  = unit conversion factor (4.73 English, 10.7 SI)

## Manning

$$K_P = \frac{C_f L n^z}{D^{5.33}} \quad (2.30)$$

where  $n$  = Manning's roughness coefficient

$z = 2$

$C_f$  = unit conversion factor [4.64 English, 10.3 SI (ASCE/WEF, 1982)]

## Minor Losses

A resistance coefficient can also be defined for minor losses, as shown in the equation below. Like the pipe resistance coefficient, the resistance coefficient for minor losses is a function of the physical characteristics of the fitting or appurtenance and the discharge.

$$h_m = K_M Q^2 \quad (2.31)$$

where  $h_m$  = head loss due to minor losses (L)

$K_M$  = minor loss resistance coefficient ( $T^2/L^5$ )

$Q$  = pipeline flow rate ( $L^3/T$ )

Solving for the minor loss resistance coefficient by substituting Equation 2.24, results in:

$$K_M = \frac{\sum K_L}{2gA^2} \quad (2.32)$$

where  $\sum K_L$  = sum of individual minor loss coefficients

## 2.7 ENERGY GAINS - PUMPS

There are many occasions when energy needs to be added to a hydraulic system to overcome elevation differences, friction losses, and minor losses. A pump is a device to which mechanical energy is applied and transferred to the water as total head. The head added is called *pump head*, and is a function of the flow rate through the pump. The following discussion is oriented toward *centrifugal pumps* since they are the most frequently used pumps in water distribution systems. Additional information about pumps can be found in Bosserman (2000), Hydraulic Institute Standards (2000), Karassik (1976), and Sanks (1998).

## Pump Head-Discharge Relationship

The relationship between pump head and pump discharge is given in the form of a *head versus discharge curve* (also called a head characteristic curve) similar to the one shown in Figure 2.13. This curve defines the relationship between the head that the pump adds and the amount of flow that the pump passes. The pump head versus discharge relationship is nonlinear, and as one would expect, the more water the pump passes, the less head it can add. The head that is plotted in the head characteristic curve is the head difference across the pump, called the *total dynamic head* (TDH).

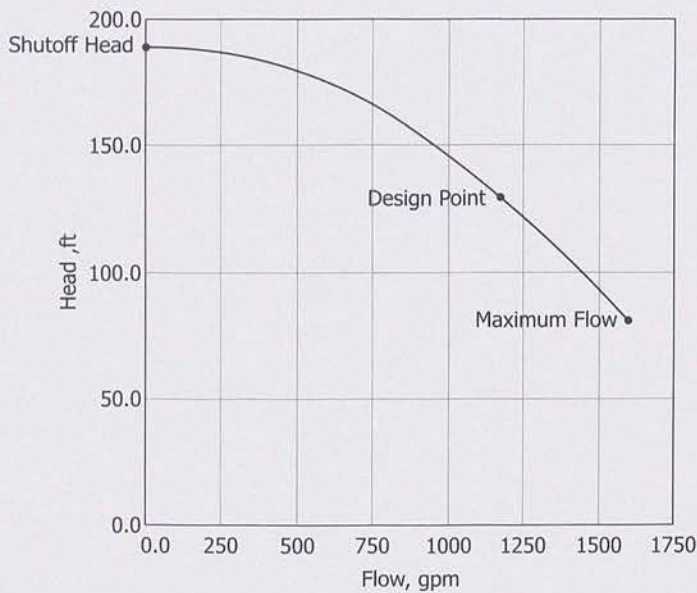
This curve must be described as a mathematical function to be used in a hydraulic simulation. Some models fit a polynomial curve to selected data points, but a more common approach is to describe the curve using a power function in the following form:

$$h_p = h_o - c Q_p^m \quad (2.33)$$

where  $h_p$  = pump head (L)  
 $h_o$  = cutoff (shutoff) head (pump head at zero flow) (L)  
 $Q_p$  = pump discharge ( $L/T^3$ )  
 $c, m$  = coefficients describing pump curve shape

More information on pump performance testing is available in Chapter 5 (see page 179).

**Figure 2.13**  
Pump head  
characteristic curve



**Affinity Laws for Variable-Speed Pumps.** A centrifugal pump's characteristic curve is fixed for a given motor speed and impeller diameter, but can be deter-

mined for any speed and any diameter by applying relationships called the *affinity laws*. For variable-speed pumps, these affinity laws are presented as:

$$Q_{P1}/Q_{P2} = n_1/n_2 \quad (2.34)$$

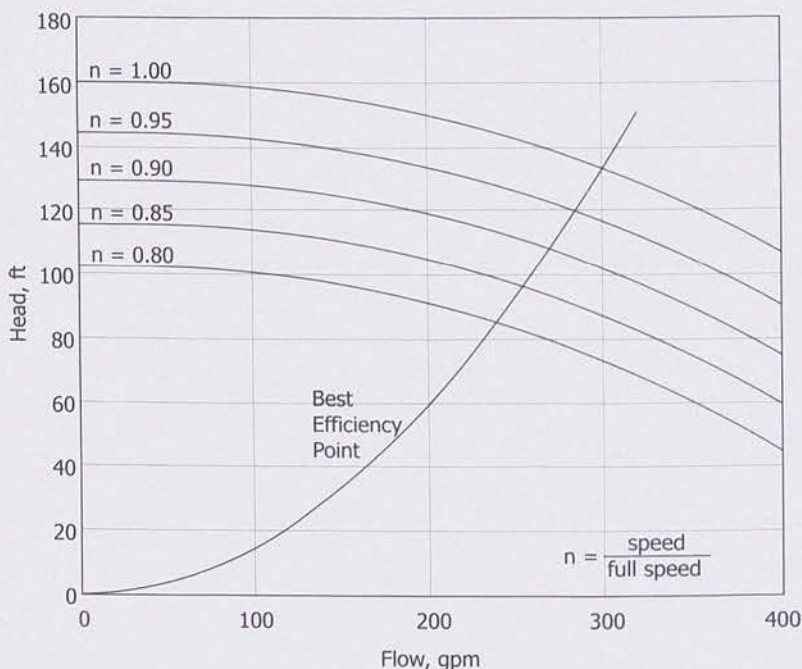
$$h_{P1}/h_{P2} = (n_1/n_2)^2 \quad (2.35)$$

where  $Q_{p1, p2}$  = pump flow rate ( $\text{L}^3/\text{T}$ )  
 $n_{1, 2}$  = pump speed ( $1/\text{T}$ )  
 $h_{p1, p2}$  = pump head (L)

Thus, pump discharge rate is directly proportional to pump speed, and pump discharge head is proportional to the square of the speed. Using this relationship, once the pump curve at any one speed is known, then the curve at another speed can be predicted. Figure 2.14 illustrates the affinity laws for variable-speed pumps where the line through the pump head characteristic curves represents the locus of best efficiency points.

**Figure 2.14**

Relative speed factors for variable-speed pumps



### System Head Curves

The purpose of a pump is to overcome elevation differences and head losses due to pipe friction and fittings. The amount of head the pump must add to overcome elevation differences is dependent on system characteristics and topology (and independent

of the pump discharge rate), and is referred to as *static head* or *static lift*. Friction and minor losses, however, are highly dependent on the rate of discharge through the pump. When these losses are added to the static head for a series of discharge rates, the resulting plot is called a *system head curve* (Figure 2.15).

The pump characteristic curve is a function of the pump and independent of the system, while the system head curve is dependent on the system and is independent of the pump. Unlike the pump curve, which is fixed for a given pump at a given speed, the system head curve is continually sliding up and down as tank water levels change and demands change. Rather than there being a unique system head curve, there is actually a family of system head curves forming a band on the graph.

For the case of a single pipeline between two points, the system head curve can be described in equation form as:

$$H = h_l + \sum K_p Q^z + \sum K_m Q^2 \quad (2.36)$$

where  $H$  = total head (L)

$h_l$  = static lift (L)

$K_p$  = pipe resistance coefficient ( $T^z/L^{3z-1}$ )

$Q$  = pipe discharge ( $L^3/T$ )

$z$  = coefficient

$K_m$  = minor loss resistance coefficient ( $T^2/L^5$ )

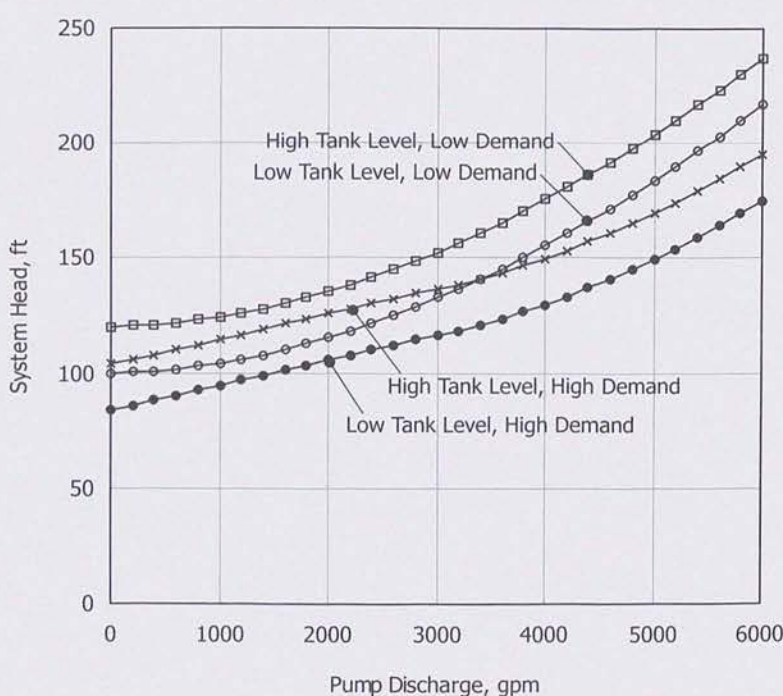


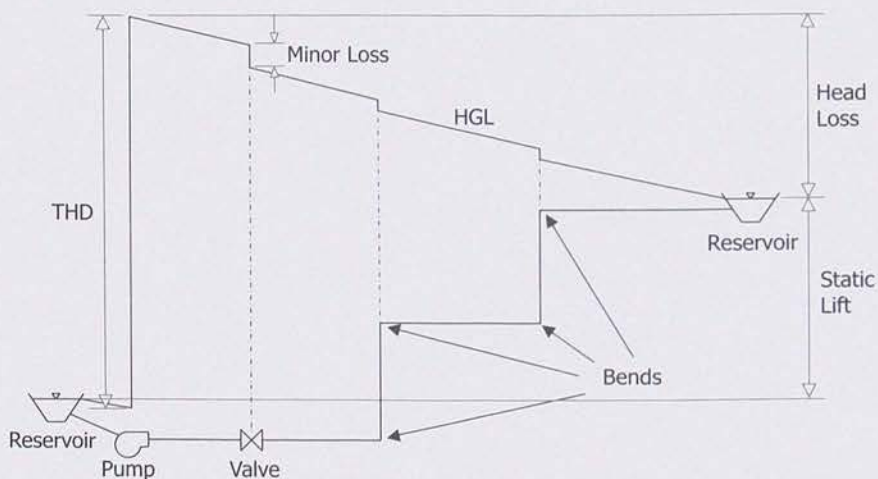
**Figure 2.15**

A family of system head curves

Thus, the head losses and minor losses associated with each segment of pipe are summed along the total length of the pipeline. When the system is more complex, the interdependencies of the hydraulic network make it impossible to write a single equation to describe a point on the system curve. In these cases, hydraulic analysis using a hydraulic model may be needed. It is helpful to visualize the hydraulic grade line as increasing abruptly at a pump and sloping downward as the water flows through pipes and valves (Figure 2.16).

**Figure 2.16**

Schematic of hydraulic grade line for a pumped system



## Pump Operating Point

When the pump head discharge curve and the system head curve are plotted on the same axes (Figure 2.17), there is only one point that lies on both the pump characteristic curve and the system head curve. This intersection defines the pump *operating point*, which represents the discharge that will pass through the pump and the head that the pump will add. This head is equal to the head needed to overcome the static head and other losses in the system.

## Other Uses of Pump Curves

In addition to the pump head-discharge curve, other curves representing pump behavior describe power, water horsepower, and efficiency (Figure 2.18), and are discussed further in Chapter 3 (see page 93) and Chapter 5 (see page 179). Since utilities want to minimize the amount of energy necessary for system operation, the engineer should select pumps that run as efficiently as possible. Pump operating costs are discussed further in Chapter 9 (see page 353).

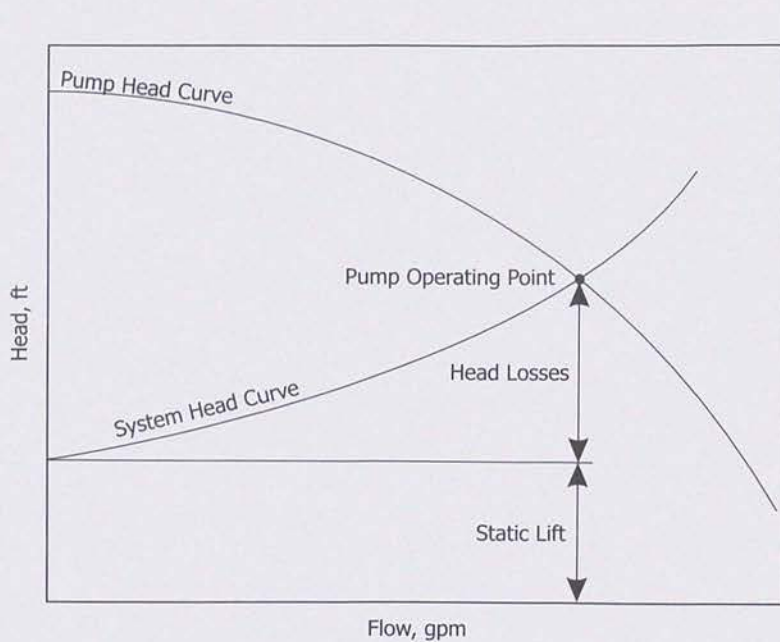


**Figure 2.17**  
System operating point

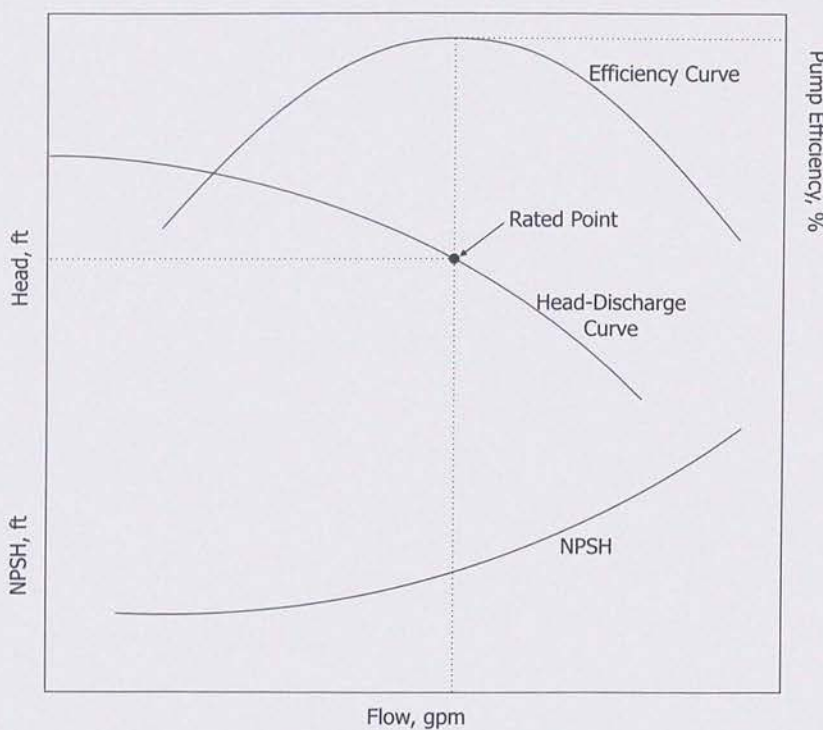


**Figure 2.18**  
Pump efficiency curve

Another issue when designing a pump is the *net positive suction head* (NPSH) required (see page 260). NPSH is the head that is present at the suction side of the pump. Each pump requires that the available NPSH exceed the required NPSH to ensure that local pressures within the pump do not drop below the vapor pressure of the fluid, causing cavitation. As discussed on page 24, cavitation is essentially a boiling of the liquid within the pump, and it can cause tremendous damage. The NPSH required is unique for each pump model, and is a function of flow rate. The use of a calibrated hydraulic model in determining available net positive suction head is discussed further on page 260.

## 2.8 NETWORK HYDRAULICS

In networks of interconnected hydraulic elements, every element is influenced by each of its neighbors; the entire system is interrelated in such a way that the condition of one element must be consistent with the condition of all other elements. Two concepts define these interconnections:

- Conservation of mass
- Conservation of energy

### Conservation of Mass

The principle of *Conservation of Mass* (Figure 2.19) dictates that the fluid mass that enters any pipe will be equal to the mass leaving the pipe (since fluid is typically neither created nor destroyed in hydraulic systems). In network modeling, all outflows are lumped at the nodes or junctions.

$$\sum_{\text{pipes}} Q_i - U = 0 \quad (2.37)$$

where  $Q_i$  = inflow to node in  $i$ -th pipe ( $\text{L}^3/\text{T}$ )  
 $U$  = water used at node ( $\text{L}^3/\text{T}$ )

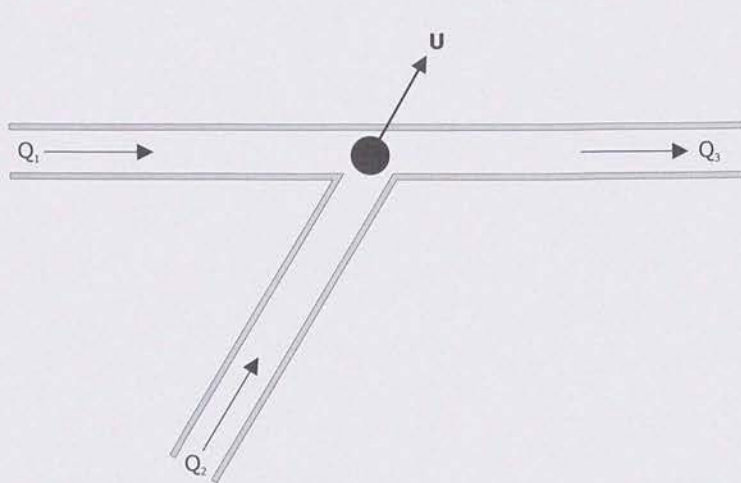
Note that for pipe outflows from the node, the sign of  $Q$  is negative.

When extended period simulations are considered, water can be stored and withdrawn from tanks, thus a term is needed to describe the accumulation of water at certain nodes:

$$\sum_{\text{pipes}} Q_i - U - \frac{dS}{dt} = 0 \quad (2.38)$$

where  $\frac{dS}{dt}$  = change in storage ( $\text{L}^3/\text{T}$ )

The conservation of mass equation is applied to all junction nodes and tanks in a network, and one equation is written for each of them.

**Figure 2.19**

Conservation of Mass principle

## Conservation of Energy

The principle of *Conservation of Energy* dictates that the difference in energy between two points must be the same regardless of the path that is taken (Bernoulli, 1738). For convenience within the hydraulic analysis, the equation is written in terms of head as:

$$Z_1 + \frac{P_1}{\gamma} + \frac{V_1^2}{2g} + \sum h_p = Z_2 + \frac{P_2}{\gamma} + \frac{V_2^2}{2g} + \sum h_L + \sum h_m \quad (2.39)$$

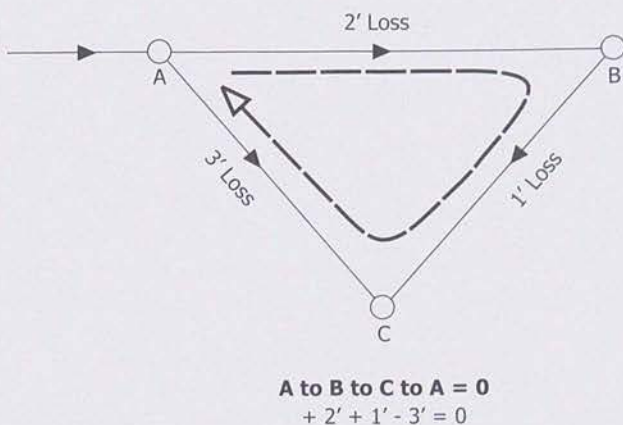
where

 $Z$  = elevation (L) $P$  = pressure ( $M/L/T^2$ ) $\gamma$  = fluid specific weight ( $M/L^2/T^2$ ) $V$  = velocity ( $L/T$ ) $g$  = gravitational acceleration constant ( $L/T^2$ ) $h_p$  = head added at pumps (L) $h_L$  = head loss in pipes (L) $h_m$  = head loss due to minor losses (L)

Thus the difference in energy at any two points connected in a network is equal to the energy gains from pumps and energy losses in pipes and fittings that occur in the path between them. This equation can be written for any open path between any two points. Of particular interest are paths between reservoirs or tanks (where the difference in head is known), or paths around loops since the changes in energy must sum to zero as illustrated in Figure 2.20.

**Figure 2.20**

The sum of head losses around a pipe loop is equal to zero



### Solving Network Problems

Real water distribution systems do not consist of a single pipe and cannot be described by a single set of continuity and energy equations. Instead, one continuity equation must be developed for each node in the system, and one energy equation must be developed for each pipe (or loop), depending on the method used. For real systems, these equations can number in the thousands.

The first systematic approach for solving these equations was developed by Hardy Cross (1936). The invention of digital computers, however, allowed more powerful numerical techniques to be developed. These techniques set up and solve the system of equations describing the hydraulics of the network in matrix form. Because the energy equations are non-linear in terms of flow and head, they cannot be solved directly. Instead, these techniques estimate a solution and then iteratively improve it until the difference between solutions falls within a specified tolerance. At this point, the hydraulic equations are considered solved.

Some of the methods used in network analysis are described in Bhave (1991); Lansey and Mays (2000); Larock, Jeppson, and Watters (1999); and Todini and Pilati (1987).

## 2.9 WATER QUALITY MODELING

*Water quality modeling* is a direct extension of hydraulic network modeling and can be used to perform many useful analyses. Developers of hydraulic network simulation models recognized the potential for water quality analysis and began adding water quality calculation features to their models in the mid 1980s. *Transport*, mixing, and *decay* are the fundamental physical and chemical processes typically represented in water quality models. Water quality simulations also use the network hydraulic solution as part of their computations. Flow rates in pipes and the flow paths that define how water travels through the network are used to determine mixing, *residence times*, and other hydraulic characteristics affecting disinfectant transport

and decay. The results of an extended period hydraulic simulation can be used as a starting point in performing a water quality analysis.

The equations describing transport through pipes, mixing at nodes, and storage and mixing in tanks are adapted from Boccelli, et al. (1998), and those describing chemical formation and decay reactions are developed in each of the following sections. Additional information on water quality models can be found in Clark and Grayman (1998) and Grayman, Rossman, and Geldreich (2000).

## Transport in Pipes

Most water quality models make use of one-dimensional advective-reactive transport to predict the changes in constituent concentrations due to transport through a pipe, and to account for formation and decay reactions. Equation 2.40 shows concentration within a pipe  $i$  as a function of distance along its length ( $x$ ) and time ( $t$ ).

$$\frac{\partial C_i}{\partial t} = \frac{Q_i}{A_i} \frac{\partial C_i}{\partial x} + \theta(C_i), i = 1 \dots P \quad (2.40)$$

where  $C_i$  = concentration in pipe  $i$  ( $M/L^3$ )

$Q_i$  = flow rate in pipe  $i$  ( $L^3/T$ )

$A_i$  = cross-sectional area of pipe  $i$  ( $L^2$ )

$\theta(C_i)$  = reaction term ( $M/L^3/T$ )

Equation 2.40 must be combined with two boundary condition equations (concentration at  $x = 0$  and  $t = 0$ ) to obtain a solution. Equation 2.40 is typically solved, however, by converting it to a standard first-order differential equation using a finite-difference scheme as shown in Equation 2.41.

$$\frac{dC_{i,l}}{dt} = \frac{Q_i}{A_i} \frac{(C_{i,l} - C_{i,l-1})}{\Delta x_i} + \theta(C_{i,l}), i = 1 \dots P, l = 1 \dots n_i \quad (2.41)$$

where  $C_{i,l}$  = concentration in pipe  $i$  at finite difference node  $l$  ( $M/L^3$ )

$\Delta x_i$  = distance between finite difference nodes ( $L$ )

$\theta(C_{i,l})$  = reaction term ( $M/L^3/T$ )

$n_i$  = number of finite difference nodes in pipe  $i$

The equation for *advective transport* is a function of the flow rate in the pipe divided by the cross-sectional area, which is equal to the mean velocity of the fluid. Thus, the bulk fluid is transported down the length of the pipe with a velocity that is directly proportional to the average flow rate. The equation is based on the assumption that longitudinal dispersion in pipes is negligible, and the bulk fluid is completely mixed (a valid assumption under turbulent conditions). Furthermore, the equation can also account for the formation or decay of a substance during transport with the substitution of a suitable equation into the reaction term. Such an equation will be developed later. First, however, the nodal mixing equation is presented.

## Mixing at Nodes

Water quality simulation uses a nodal mixing equation to combine concentrations from individual pipes described by the advective transport equation, and to define the boundary conditions for each pipe as referred to above. The equation is written by performing a mass balance on concentrations entering a junction node.

$$C_{OUT_j} = \frac{\sum_{i \in IN_j} Q_i C_{i,n_i} + U_j}{\sum_{i \in OUT_j} Q_i} \quad (2.42)$$

where  $C_{OUT_j}$  = concentration leaving the junction node  $j$  ( $M/L^3$ )

$OUT_j$  = set of pipes leaving node  $j$

$IN_j$  = set of pipes entering node  $j$

$Q_i$  = flow rate entering the junction node from pipe  $i$  ( $L^3/T$ )

$C_{i,n_i}$  = concentration entering junction node from pipe  $i$  ( $M/L^3$ )

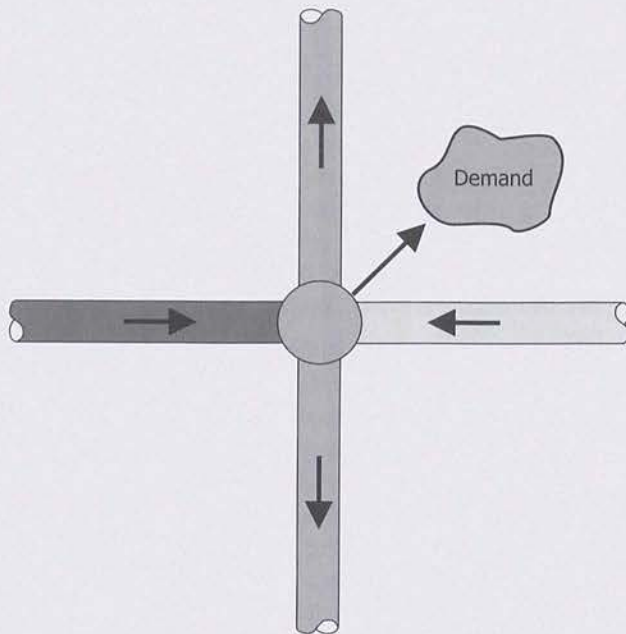
$U_j$  = concentration source at junction node  $j$  ( $M/T$ )

The nodal mixing equation describes the concentration leaving a network node (either by advective transport into an adjoining pipe or by removal from the network as a demand) as a function of the concentrations that enter it. The equation describes the flow-weighted average of the incoming concentrations. If a source is located at a junction, constituent mass can also be added and combined in the mixing equation

with the incoming concentrations. Figure 2.21 illustrates how the nodal mixing equation is used at a pipe junction. Concentrations enter the node with pipe flows. The incoming concentrations are mixed according to Equation 2.42, and the resulting concentration is transported through the outgoing pipes and as demand leaving the system. The nodal mixing equation assumes that incoming flows are completely and instantaneously mixed. The basis for the assumption is the turbulence occurring at the junction node, which is usually sufficient for good mixing.

**Figure 2.21**

Nodal mixing



## Mixing in Tanks

Pipes are sometimes connected to reservoirs and tanks as opposed to junction nodes. Again, a mass balance of concentrations entering or leaving the tank or reservoir can be performed.

$$\frac{dC_k}{dt} = \frac{Q_i}{V_k}(C_{i,np}(t) - C_k) + \theta(C_k) \quad (2.43)$$

where  $C_k$  = concentration within tank or reservoir  $k$  ( $\text{M/L}^3$ )

$Q_i$  = flow entering the tank or reservoir from pipe  $i$  ( $\text{L}^3/\text{T}$ )

$V_k$  = volume in tank or reservoir  $k$  ( $\text{L}^3$ )

$\theta(C_k)$  = reaction term ( $\text{M/L}^3/\text{T}$ )

Equation 2.43 applies when a tank is filling. During a hydraulic time step in which the tank is filling, the water entering from upstream pipes mixes with water that is already in storage. If the concentrations are different, blending occurs. The tank mixing equation accounts for blending and any reactions that occur within the tank volume during

the hydraulic step. During a hydraulic step in which draining occurs, terms can be dropped and the equation simplified.

$$\frac{dC_k}{dt} = \theta(C_k) \quad (2.44)$$

Specifically, the dilution term can be dropped since it does not occur. Thus, the concentration within the volume is only subject to chemical reactions. Furthermore, the concentration draining from the tank becomes a boundary condition for the advective transport equation written for the pipe connected to it.

Equations 2.43 and 2.44 assume that concentrations within the tank or reservoir are completely and instantaneously mixed. This assumption is frequently applied in water quality models. There are, however, other useful mixing models for simulating flow processes in tanks and reservoirs (Grayman, et al., 1996). For example, contact basins or clear wells designed to provide sufficient contact time for disinfectants are frequently represented as simple plug-flow reactors using a “first in first out” (FIFO) model. In a FIFO model, the first volume of water to enter the tank during a filling cycle is the first to leave during the drain cycle.

If severe short-circuiting is occurring within the tank, a “last in first out” (LIFO) model should be applied, in which the first volume entering the tank during filling is the last to leave while draining. More complex tank mixing behavior can be captured using more generalized “compartment” models. *Compartment models* have the ability to represent mixing processes and time delays within tanks more accurately. Figure 2.22 illustrates a three-compartment model for a tank with a single pipe for filling and draining. Good quality water entering the tank occupies the first compartment, and a mixing zone and poor quality water are found in compartments two and three, respectively. The model simulates the exchange of water between different compartments, and in doing so, mimics complex tank mixing dynamics. All of the models mentioned above can be used to simulate a non-reactive (conservative) constituent, as well as decay or formation reactions for substances that react over time.

## Chemical Reaction Terms

Equations 2.41, 2.42, 2.43, and 2.44 compose the linked system of first-order differential equations solved by typical water quality simulation algorithms. This set of equations and the algorithms for solving them can be used to model different chemical reactions known to impact water quality in distribution systems. Chemical reaction terms are present in Equations 2.41, 2.43, and 2.44. Concentrations within pipes, storage tanks, and reservoirs are a function of these reaction terms. Once water leaves the treatment plant and enters the distribution system, it is subject to many complex physical and chemical processes, some of which are poorly understood, and most of which are not modeled. Three chemical processes that are frequently modeled, however, are bulk fluid reactions, reactions that occur on a surface (typically the pipe wall), and formation reactions involving a limiting reactant. First, an expression for bulk fluid reactions is presented, and then a reaction expression that incorporates both bulk and pipe wall reactions is developed.

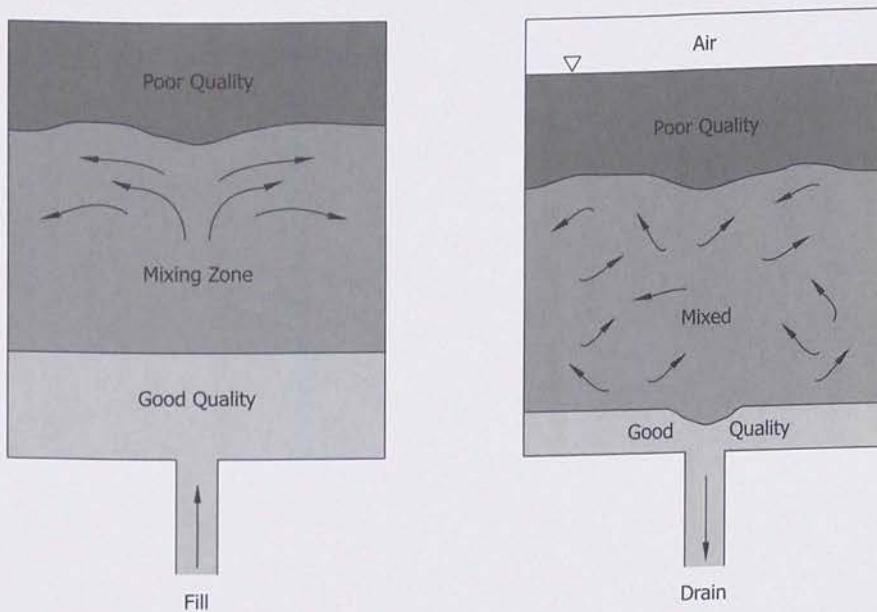


**Figure 2.22**  
Three-compartment tank mixing model

**Bulk Reactions.** Bulk fluid reactions occur within the fluid volume and are a function of constituent concentrations, reaction rate and order, and concentrations of the formation products. A generalized expression for  $n^{\text{th}}$  order bulk fluid reactions is developed in Equation 2.45 (Rossman, 2000).

$$\theta(C) = \pm kC^n \quad (2.45)$$

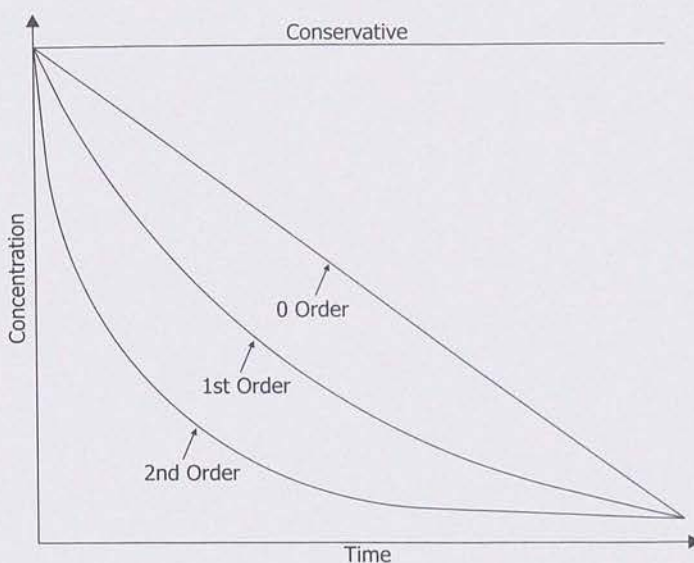
where  $\theta(C)$  = reaction term ( $M/L^3/T$ )  
 $k$  = reaction rate coefficient  $[(L^3/M)^{n-1}/T]$   
 $C$  = concentration ( $M/L^3$ )  
 $n$  = reaction rate order constant

Equation 2.45 is the generalized bulk reaction term most frequently used in water quality simulation models. The rate expression only accounts for a single reactant concentration, tacitly assuming that any other reactants (if they participate in the reaction) are available in excess of the concentration necessary to sustain the reaction. The sign of the *reaction rate coefficient*,  $k$ , signifies that a *formation reaction* (positive) or a *decay reaction* (negative) is occurring. The units of the reaction rate coefficient depend on the order of the reaction. The order of the reaction depends on the composition of the reactants and products that are involved in the reaction. The reaction rate order is frequently determined experimentally.

*Zero-, first-, and second-order decay reactions* are commonly used to model chemical processes that occur in distribution systems. Figure 2.23 is a conceptual illustration showing the change in concentration versus time for these three most common reaction rate orders. Using the generalized expression in Equation 2.45, these reactions can be modeled by allowing  $n$  to equal 0, 1, or 2, and then performing a regression analysis to experimentally determine the rate coefficient.

**Figure 2.23**

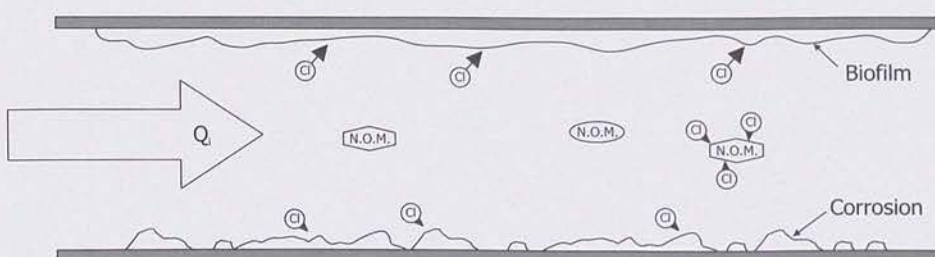
Conceptual illustration of concentration vs. time for zero, first, and second-order decay reactions



**Bulk and Wall Reactions.** Disinfectants are the most frequently modeled constituents in water distribution systems. Upon leaving the plant and entering the distribution system, disinfectants are subject to a poorly characterized set of potential chemical reactions. Figure 2.24 illustrates the flow of water through a pipe and the types of chemical reactions with disinfectants that can occur along its length. Chlorine (the most common disinfectant) is shown reacting in the bulk fluid with *natural organic matter* (NOM), and at the pipe wall, where oxidation reactions with biofilms and the pipe material (a cause of corrosion) can occur.

**Figure 2.24**

Disinfectant reactions occurring within a typical distribution system pipe



Many disinfectant decay models have been developed to account for these reactions. The first-order decay model has been shown to be sufficiently accurate for most distribution system modeling applications and is well established. Rossman, Clark, and Grayman (1994) proposed a mathematical framework for combining the complex reactions occurring within distribution system pipes. This framework accounts for the physical transport of the disinfectant from the bulk fluid to the pipe wall (mass transfer effects) and the chemical reactions occurring there.

$$\theta(C) = \pm KC \quad (2.46)$$

where  $K$  = overall reaction rate constant (1/T)

Equation 2.46 is a simple first-order reaction ( $n = 1$ ). The reaction rate coefficient  $K$ , however, is now a function of the bulk reaction coefficient and the wall reaction coefficient, as indicated in the following equation.

$$K = k_b + \frac{k_w k_f}{R_H(k_w + k_f)} \quad (2.47)$$

where  $k_b$  = bulk reaction coefficient (1/T)

$k_w$  = wall reaction coefficient (L/T)

$k_f$  = mass transfer coefficient, bulk fluid to pipe wall (L/T)

$R_H$  = hydraulic radius of pipeline (L)

The rate that disinfectant decays at the pipe wall depends on how quickly disinfectant is transported to the pipe wall and the speed of the reaction once it is there. The mass transfer coefficient is used to determine the rate at which disinfectant is transported using the dimensionless *Sherwood Number*, along with the molecular diffusivity coefficient (of the constituent in water) and the pipeline diameter.

$$k_f = \frac{S_H d}{D} \quad (2.48)$$

where  $S_H$  = Sherwood number

$d$  = molecular diffusivity of constituent in bulk fluid (L<sup>2</sup>/T)

$D$  = pipeline diameter (L)

For stagnant flow conditions ( $Re < 1$ ), the Sherwood number,  $S_H$ , is equal to 2.0. For turbulent flow ( $Re > 2,300$ ), the Sherwood Number is computed using Equation 2.49.

$$S_H = 0.023 Re^{0.83} \left( \frac{v}{d} \right)^{0.333} \quad (2.49)$$

where  $Re$  = Reynolds number

$v$  = kinematic viscosity of fluid (L<sup>2</sup>/T)

For laminar flow conditions ( $1 < Re < 2,300$ ), the average Sherwood Number along the length of the pipe can be used. To have laminar flow in a 6-in. (150-mm) pipe, the flow would need to be less than 5 gpm (0.3 l/s) with a velocity of 0.056 ft/s (0.017 m/s). At such flows, head loss would be negligible.

$$S_H = 3.65 + \frac{0.0668 \left( \frac{D}{L} \right) (Re) \left( \frac{v}{d} \right)}{1 + 0.04 \left[ \left( \frac{D}{L} \right) Re \left( \frac{v}{d} \right) \right]^{2/3}} \quad (2.50)$$

where  $L$  = pipe length (L)

Using the first-order reaction framework developed immediately above, both bulk fluid and pipe wall disinfectant decay reactions can be accounted for. Bulk decay coefficients can be determined experimentally. *Wall decay coefficients*, however, are more difficult to measure and are frequently estimated using disinfectant concentration field measurements and water quality simulation results.

**Formation Reactions.** One shortcoming of the first-order reaction model is that it only accounts for the concentration of one reactant. This model is sufficient if only one reactant is being considered. For example, when chlorine residual concentrations are modeled, chlorine is assumed to be the limiting reactant and the other reactants - material at the pipe walls and *natural organic matter* (NOM) - are assumed to be present in excess. The behavior of some *disinfection by-product* (DBP) formation reactions, however, differs from this assumption. NOM, not chlorine, is frequently the limiting reactant. DBP formation is just one example of a generalized class of reactions that can be modeled using a limiting reactant. The reaction term for this class of formation and decay reactions as proposed by Rossman (2000) is shown in Equation 2.51.

$$\theta(C) = \pm k(C_{lim} - C)^{n-1} \quad (2.51)$$

where  $C_{lim}$  = limiting concentration of the reaction (M/L<sup>3</sup>)

## Other Types of Water Quality Simulations

While the water quality features of individual software packages vary, the most common types of water quality simulations, in addition to the constituent analysis already described, are source trace and water age analyses. The solution methods used in both of these simulations are actually specific applications of the method used in constituent analysis.

**Source Trace Analysis.** For the sake of reliability, or to simply provide sufficient quantities of water to customers, a utility often uses more than one water supply source. Suppose, for instance, that two treatment plants serve the same distribution system. One plant draws water from a surface source, and the other pulls from an underground aquifer. The raw water qualities from these sources are likely to differ significantly, resulting in quality differences in the finished water as well.

Using a *source trace analysis*, the areas within the distribution system influenced by a particular source can be determined, and, more importantly, areas where mixing of water from different sources has occurred can be identified. The significance of source mixing is dependent upon the quality characteristics of the waters. Sometimes, mixing can reduce the aesthetic qualities of the water (for example, creating cloudiness as solids precipitate, or causing taste and odor problems to develop), and can contribute to disinfectant residual maintenance problems. Source trace analyses are also useful in tracking water quality problems related to storage tanks by tracing water from storage as it is transported through the network.

A source trace analysis is a useful tool for better management of these situations. Specifically, it can be used to determine the percentage of water originating from a particular source for each junction node, tank, and reservoir in the distribution system model. The procedure the software uses for this calculation is a special case of constituent analysis in which the trace originates from the source as a conservative constituent with an output concentration of 100 units. The constituent transport and mixing equations introduced in the beginning of this section are then used to simulate

the transport pathways through the network and the influence of transport delays and dilution on the trace constituent concentration. The values computed by the simulation are then read directly as the percentage of water arriving from the source location.

**Water Age Analysis.** The chemical processes that can affect distribution system water quality are a function of water chemistry and the physical characteristics of the distribution system itself (for example, pipe material and age). More generally, however, these processes occur over time, making residence time in the distribution system a critical factor influencing water quality. The cumulative residence time of water in the system, or *water age*, has come to be regarded as a reliable surrogate for water quality. Water age is of particular concern when quantifying the effect of storage tank turnover on water quality. It is also beneficial for evaluating the loss of disinfectant residual and the formation of disinfection by-products in distribution systems.

The chief advantage of a water age analysis when compared to a constituent analysis is that once the hydraulic model has been calibrated, no additional water quality calibration procedures are required. The water age analysis, however, will not be as precise as a constituent analysis in determining water quality; nevertheless, it is an easy way to leverage the information imbedded in the calibrated hydraulic model. Consider a project in which a utility is analyzing mixing in a tank and its effect on water quality in an area of a network experiencing water quality problems. If a hydraulic model has been developed and adequately calibrated, it can immediately be used to evaluate water age. The water age analysis may indicate that excessively long residence times within the tank are contributing to water quality degradation. Using this information, a more precise analysis can be planned (such as an evaluation of tank hydraulic dynamics and mixing characteristics, or a constituent analysis to determine the impact on disinfectant residuals), and preliminary changes in design or operation can be evaluated.

The water age analysis reports the cumulative residence time for each parcel of water moving through the network. Again, the algorithm the software uses to perform the analysis is a specialized case of constituent analysis. Water entering a network from a source is considered to have an age of zero. The constituent analysis is performed assuming a zero-order reaction with a  $k$  value equal to  $+1 \text{ [(l/mg)/s]}$ . Thus, constituent concentration growth is directly proportional to time, and the cumulative residence time along the transport pathways in the network is numerically summed.

Using the descriptions of water quality transport and reaction dynamics provided here, and the different types of water quality-related simulations available in modern software packages, water quality in the distribution system can be accurately predicted. Water quality modeling can be used to help improve the performance of distribution system modifications meant to reduce hydraulic residence times, and as a tool for improving the management of disinfectant residuals and other water quality-related operations. Continuing advancements in technology combined with more stringent regulations on quality at the customer's tap are motivating an increasing number of utilities to begin using the powerful water quality modeling capabilities already available to them.

## REFERENCES

---

- Almeida, A. B., and Koelle, E. (1992). *Fluid Transients in Pipe Networks*. Elsevier Applied Science, Southampton, UK.
- ASCE. (1975). *Pressure Pipeline Design for Water and Wastewater*. ASCE, New York, New York.
- ASCE/WEF. (1982). *Gravity Sanitary Sewer Design and Construction*. ASCE, Reston, Virginia.
- ASCE Committee on Pipeline Planning. (1992). *Pressure Pipeline Design for Water and Wastewater*. ASCE, Reston, Virginia.
- Bernoulli, D. (1738). *Hydrodynamica*. Argentorati.
- Bhave, P. R. (1991). *Analysis of Flow in Water Distribution Networks*. Technomics, Lancaster, Pennsylvania.
- Boccelli, D. L., Tryby, M. E., Uber, J. G., Rossman, L. A., Zierolf, M. L., and Polycarpou, M. M. (1998). "Optimal Scheduling of Booster Disinfection in Water Distribution Systems." *Journal of Water Resources Planning and Management*, ASCE, 124(2), 99.
- Bosserman, B. E., (2000). "Pump System Hydraulic Design." *Water Distribution System Handbook*, Mays, L. W., ed., McGraw-Hill, New York, New York.
- Chaudhry, M. H. (1987). *Applied Hydraulic Transients*. Van Nostrand Reinhold, New York.
- Clark, R. M., and Grayman, W. M. (1998). *Modeling Water Quality in Distribution Systems*. AWWA, Denver, Colorado.
- Crane Company (1972). *Flow of Fluids through Valves and Fittings*. Crane Co., New York, New York.
- Cross, H. (1936). "Analysis of Flow in Networks of Conduits or Conductors." *Univ. Of Illinois Experiment Station Bulletin No. 286*, Department of Civil Engineering, University of Illinois, Champaign Urbana, Illinois.
- Grayman, W. M., Deininger, R. A., Green, A., Boulos, P. F., Bowcock, R. W., and Godwin, C. C. (1996). "Water Quality and Mixing Models for Tanks and Reservoirs." *Journal of the American Water Works Association*, 88(7).
- Grayman, W. M.; Rossman, L. A., and Geldreich, E. E. (2000). "Water Quality." *Water Distribution Systems Handbook*, Mays, L. W., ed., McGraw-Hill, New York, New York.
- Hydraulic Institute (2000). *Pump Standards*. Parsippany, New Jersey.
- Idelchik, I. E. (1999). *Handbook of Hydraulic Resistance*. 3rd edition. Begell House, New York, New York.
- Karney, B. W. (2000). "Hydraulics of Pressurized Flow." *Water Distribution Systems Handbook*, Mays, L.W., ed., McGraw-Hill, New York.
- Lamont, P. A. (1981). "Common Pipe Flow Formulas Compared with the Theory of Roughness." *Journal of the American Water Works Association*, 73(5), 274.
- Lansey, K., and Mays, L. W. (2000). "Hydraulics of Water Distribution Systems." *Water Distribution Systems Handbook*, Mays, L. W., ed., McGraw-Hill, New York, New York.
- Larock, B. E., Jeppson, R. W., and Watters, G. Z. (1999). *Handbook of Pipeline Systems*. CRC Press, Boca Raton, Florida.
- Karassik, I. J., ed. (1976). *Pump Handbook*. McGraw-Hill, New York, New York.
- Martin, C. S. (2000). "Hydraulic Transient Design for Pipeline Systems." *Water Distribution Systems Handbook*, Mays, L.W., ed., McGraw-Hill, New York, New York.
- Mays, L. W., ed. (1999). *Hydraulic Design Handbook*. McGraw-Hill, New York, New York.
- Miller, D. S. (1978). *Internal Flow Systems*. BHRA Fluid Engineering, Bedford, United Kingdom.
- Moody, L. F. (1944). "Friction Factors for Pipe Flow." *Transactions of the American Society of Mechanical Engineers*, Vol. 66.

- Nikuradse (1932). "Gesetzmassigkeiten der Turbulenten Stromung in Glatten Rohren." *VDI-Forschungsh.*, No. 356 (in German).
- Rossman, L. A., Clark, R. M., and Grayman, W. M. (1994). "Modeling Chlorine Residuals in Drinking Water Distribution Systems." *Journal of Environmental Engineering*, ASCE, 1210(4), 803.
- Rossman, L.A. (2000). *EPANET Users Manual*. Risk Reduction Engineering Laboratory, U.S. Environmental Protection Agency, Cincinnati, Ohio.
- Sanks, R. L., ed. (1998). *Pumping Station Design*. 2nd edition, Butterworth, London, UK.
- Streeter, V. L., Wylie, B. E., and Bedford, K. W. (1998). *Fluid Mechanics*. 9th edition, WCB/McGraw-Hill, Boston, Massachusetts.
- Swamee, P. K., and Jain, A. K. (1976). "Explicit Equations for Pipe Flow Problems." *Journal of Hydraulic Engineering*, ASCE, 102(5), 657.
- Thorley, A. R. D. (1991). *Fluid Transients in Pipeline Systems*. D&L George Ltd., UK.
- Todini, E., and Pilati, S. (1987). "A Gradient Method for the Analysis of Pipe Networks." *Proceedings of the International Conference on Computer Applications for Water Supply and Distribution*, Leicester Polytechnic, UK.
- Walski, T. M. (1984). *Analysis of Water Distribution Systems*. Van Nostrand Reinhold, New York, New York.
- Williams, G. S., and Hazen, A. (1920). *Hydraulic Tables*. John Wiley & Sons, New York, New York.
- Wylie, E. B., and Streeter, V. L. (1993). *Fluid Transients in Systems*. Prentice-Hall, New York.

## DISCUSSION TOPICS AND PROBLEMS

Earn  
CEUs

Read Chapters 1 and 2 and complete the problems. Submit your work to Haestad Methods and earn up to 1.5 CEUs.  
See *Continuing Education Units* on page xiii for more information, or visit [www.haestad.com/wdm-ceus/](http://www.haestad.com/wdm-ceus/).

- 2.1** Find the viscosity of the fluid contained between the two square plates shown in Figure 2.25. The top plate is moving at a velocity of 3 ft/s.

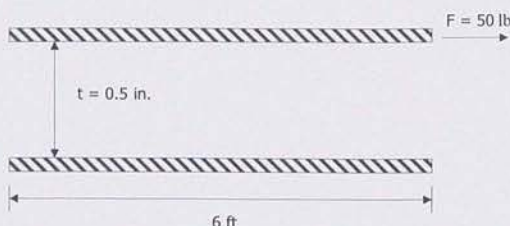


**Figure 2.25**

- 2.2** Find the force  $P$  required to pull the 150 mm circular shaft in Figure 2.26 through the sleeve at a velocity of 1.5 m/s. The fluid between the shaft and the sleeve is water at a temperature of 15°C.

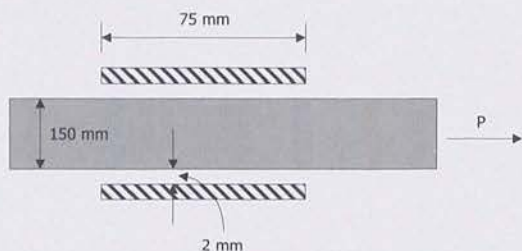
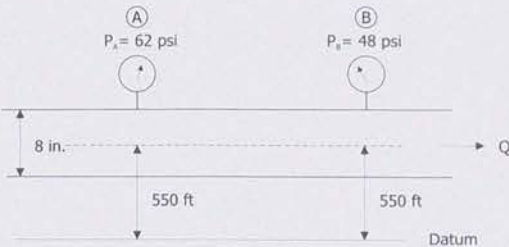


**Figure 2.26**

- 2.3** Find the pressure at the base of a container of water having a depth of 15 m.
- 2.4** How high is the water level from the base of an elevated storage tank if the pressure at the base of the tank is 45 psi?
- 2.5** Water having a temperature of 65°F is flowing through a 6-in. ductile iron main at a rate of 300 gpm. Is the flow laminar, turbulent, or transitional?
- 2.6** What type of flow do you think normally exists in water distribution systems: laminar, turbulent, or transitional? Justify your selection with sound reasoning.

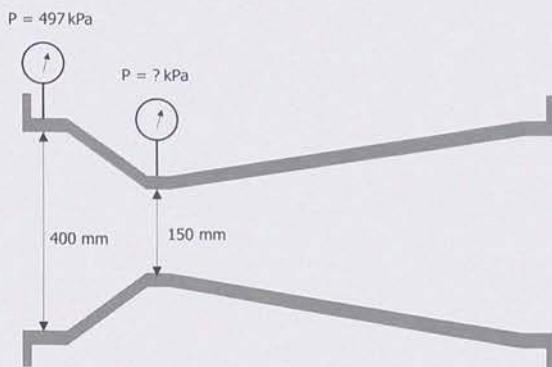
- 2.7** What is the total head at point A in the system shown in Figure 2.27 if the flow through the pipeline is 1,000 gpm? What is the head loss in feet between point A and point B?

**Figure 2.27**



- 2.8** For the piping system shown in Figure 2.27, what would the elevation at point B have to be in order for the reading on the two pressure gages to be the same?
- 2.9** Assuming that there are no head losses through the Venturi meter shown in Figure 2.28, what is the pressure reading in the throat section of the Venturi? Assume that the discharge through the meter is 158 l/s.

**Figure 2.28**



- 2.10** What is the head loss through a 10-in. diameter concrete water main 2,500 ft in length if water at 60°F is flowing through the line at a rate of 1,250 gpm? Solve using the Darcy-Weisbach formula.
- 2.11** For Problem 2.10, what is the flow through the line if the head loss is 32 ft? Solve using the Darcy-Weisbach formula.
- 2.12** Find the length of a pipeline that has the following characteristics:  $Q=41 \text{ l/s}$ ,  $D=150 \text{ mm}$ , Hazen Williams  $C=110$ ,  $H_l=7.6 \text{ m}$ .
- 2.13** For the pipeline shown in Figure 2.27, what is the Hazen-Williams C-factor if the distance between the two pressure gages is 725 ft and the flow is 1,000 gpm?

**2.14 English Units** - Compute the pipe resistance coefficient,  $K_p$ , for the following pipelines.

Length (ft)	Diameter (in.)	Hazen-Williams C-factor	Pipe Resistance Coefficient ( $K_p$ )
1,200	12	120	
500	4	90	
75	3	75	
3,500	10	110	
1,750	8	105	

*SI Units* - Compute the pipe resistance coefficient,  $K_p$ , for the following pipelines.

Length (m)	Diameter (mm)	Hazen-Williams C-factor	Pipe Resistance Coefficient ( $K_p$ )
366	305	120	
152	102	90	
23	76	75	
1067	254	110	
533	203	105	

**2.15 English Units** - Compute the minor loss term,  $K_M$ , for the fittings shown in the table below.

Type of Fitting/Flow Condition	Minor Loss Coefficient	Pipe Size (in.)	Minor Loss Term ( $K_M$ )
Gate Valve - 50% Open	4.8	8	
Tee - Line Flow	0.4	12	
90° Mitered Bend	0.8	10	
Fire Hydrant	4.5	6	

*SI Units* - Compute the minor loss term,  $K_M$ , for the fittings shown in the table below.

Type of Fitting/Flow Condition	Minor Loss Coefficient	Pipe Size (mm)	Minor Loss Term ( $K_M$ )
Gate Valve - 50% Open	4.8	200	
Tee - Line Flow	0.4	300	
90° Mitered Bend	0.8	250	
Fire Hydrant	4.5	150	

**2.16 English Units** - Determine the pressures at the following locations in a water distribution system, assuming that the HGL and ground elevations at the locations are known.

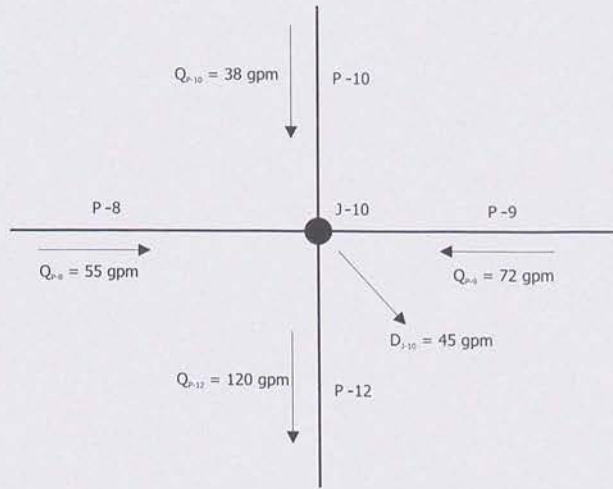
Node Label	HGL (ft)	Elevation (ft)	Pressure (psi)
J-1	550.6	423.5	
J-6	485.3	300.5	
J-23	532.6	500.0	
J-5	521.5	423.3	
J-12	515.0	284.0	

*SI Units* - Determine the pressures at the following locations in a water distribution system, assuming that the HGL and ground elevations at the locations are known.

Node Label	HGL (m)	Elevation (m)	Pressure (kPa)
J-1	167.8	129.1	
J-6	147.9	91.6	
J-23	162.3	152.4	
J-5	159.0	129.0	
J-12	157.0	86.6	

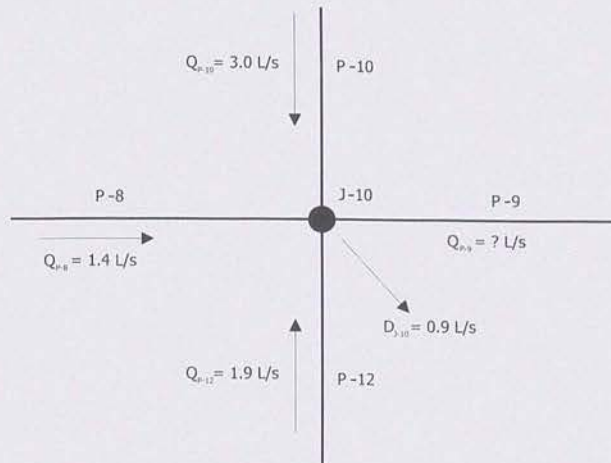
- 2.17** Using the concept of Conservation of Mass, is continuity maintained at the junction node shown in Figure 2.29?

**Figure 2.29**

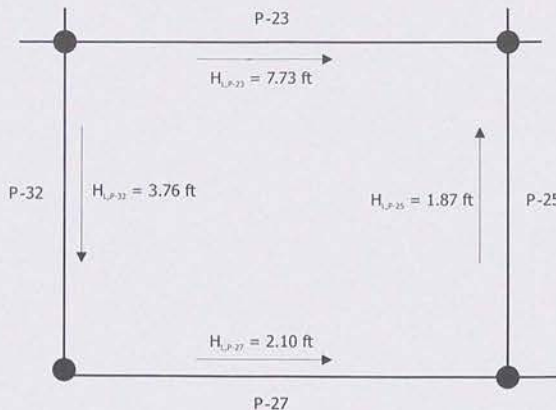


- 2.18** Find the magnitude and direction of the flow through pipe P-9 so that continuity is maintained at node J-10 in Figure 2.30.

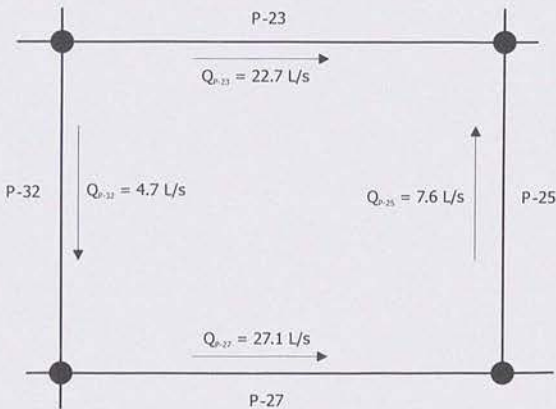
**Figure 2.30**



- 2.19** Does Conservation of Energy around a loop apply to the loop shown in the Figure 2.31? Why or why not? The total head loss (sum of friction losses and minor losses) in each pipe and the direction of flow are shown in the figure.

**Figure 2.31**

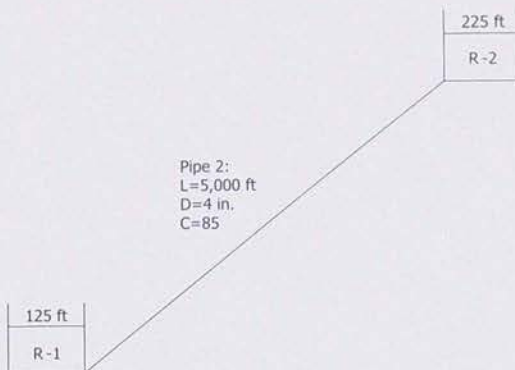
- 2.20** Does Conservation of Energy apply to the system shown in the Figure 2.32? Data describing the physical characteristics of each pipe are presented in the table below. Assume that there are no minor losses in this loop.

**Figure 2.32**

Pipe Label	Length (m)	Diameter (mm)	Hazen-Williams C-factor
P-23	381.0	305	120
P-25	228.6	203	115
P-27	342.9	254	120
P-32	253.0	152	105

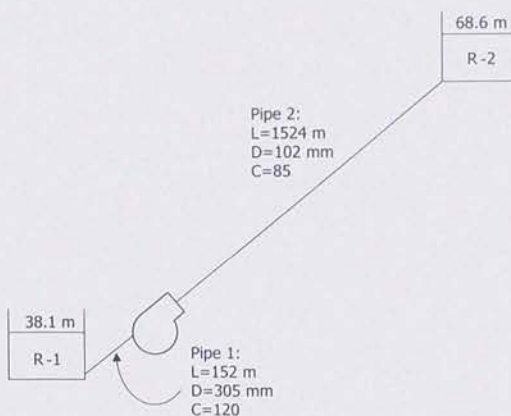
- 2.21** Find the discharge through the system shown in Figure 2.33. Compute friction loss using the Hazen-Williams equation.

**Figure 2.33**



- 2.22** Find the pump head needed to deliver water from reservoir R-1 to reservoir R-2 in Figure 2.34 at a rate of 70.8 l/s. Compute friction losses using the Hazen-Williams equation.

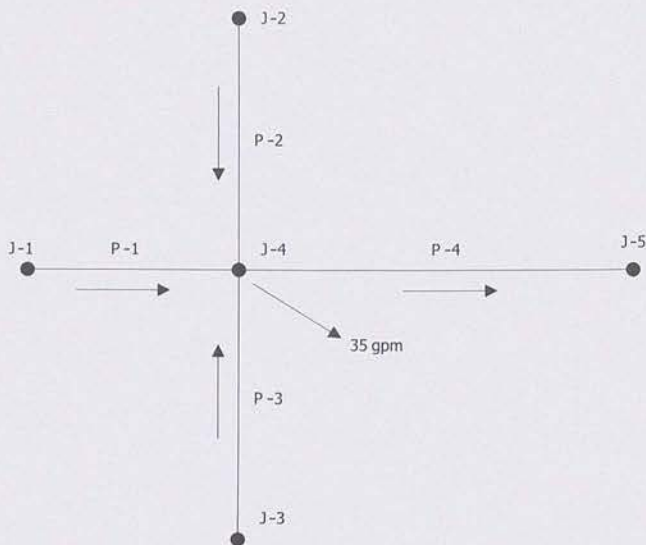
**Figure 2.34**



- 2.23** Compute the age of water at the end of a 12-in. pipe that is 1,500 ft in length and has a flow of 900 gpm. The age of the water when it enters the pipeline is 7.2 hours.

- 2.24** Suppose that a 102-mm pipe is used to serve a small cluster of homes at the end of a long street. If the length of the pipe is 975 m, what is the age of water leaving it if the water had an age of 6.3 hours when entering the line? Assume that the water use is 1.6 l/s.

- 2.25** Given the data in the tables below, what is the average age of the water leaving junction node J-4 shown in Figure 2.25? What is the flow rate through pipe P-4? What is the average age of the water arriving at node J-5 through pipe P-4? Fill in your answers in the tables provided.



Pipe Label	Flow (gpm)	Length (ft)	Diameter (in)
P-1	75	1,650	10
P-2	18	755	8
P-3	23	820	6
P-4		2,340	10

Node Label	Average Age (hours)
J-1	5.2
J-2	24.3
J-3	12.5
J-4	
J-5	

- 2.26** What will be the concentration of chlorine in water samples taken from a swimming pool after 7 days if the initial chlorine concentration in the pool was 1.5 mg/l? Bottle tests performed on the pool water indicate that the first-order reaction rate is  $-0.134 \text{ day}^{-1}$ .
- 2.27** Do you think that the actual reaction rate coefficient for water in the swimming pool described above (i.e., the water being considered remains in the pool, and is not being stored under laboratory conditions) would be equal to  $-0.134 \text{ day}^{-1}$ ? Suggest some factors that might cause the actual reaction rate to differ. Would these factors most likely cause the actual reaction rate to be greater than or less than  $-0.134 \text{ day}^{-1}$ ?

- 2.28** For the system presented in Problem 2.25, what is the concentration of a constituent leaving node J-4 (assume it is a conservative constituent)? The constituent concentration is 0.85 mg/L in pipe P-1, 0.50 mg/l in pipe P-2, and 1.2 mg/l in pipe P-3.
- 2.29** What is the fluoride concentration at the end of a 152-mm diameter pipeline 762 m in length if the fluoride concentration at the start of the line is 1.3 mg/l? Fluoride is a conservative species; that is, it does not decay over time. Ignoring dispersion, if there is initially no fluoride in the pipe and it is introduced at the upstream end at a 2.0 mg/l concentration, when will this concentration be reached at the end of the line if the flow through the pipe is 15.8 l/s? Assume that there are no other junction nodes along the length of this pipe.